Botanica Pacifica. A journal of plant science and conservation. 2025. 14(2): 11–34
DOI: 10.17581/bp.2025.14214

RESEARCH PAPER

Ontogenetic trends in the structure of the phloem rays of *Betula ermanii* (Betulaceae) in volcanic and non-volcanic environments: adaptive and functional implications

Anna V. Kopanina*, Anastasia I. Talskikh & Inna I. Vlasova

Anna V. Kopanina *
e-mail: anna.kopanina@gmail.com

Anastasia I. Talskikh
e-mail: anastasiya_talsk@mail.ru

Inna I. Vlasova
e-mail: iivlasova@gmail.com

Institute of Marine Geology and Geophysics FEB RAS, Yuzhno-Sakhalinsk, Russia

* corresponding author

Manuscript received: 16.11.2024
Review completed: 28.09.2025
Accepted for publication: 26.10.2025
Published online: 01.11.2025

ABSTRACT

We performed a comparative ontogenetic analysis (1–112 yr) of inner bark phloem parenchyma in *Betula ermanii* from typical environments on Sakhalin Island and thermal springs of Baransky Volcano, Iturup Island. A direct positive allometric correlation was observed between tree habitus and phloem radial traits. Stem diameter increased logarithmically with high coefficients of determination, while age trends of phloem ray traits followed a logarithmic pattern in young bark (up to 25–35 yr) and plateaued in mature bark. During ontogeny, the total number of rays decreased threefold, uniseriate rays by 6–9 times, ray composition shifted from 10 yr onward, and ray width increased. In volcanic environments, growth of mature trunks was reduced compared with typical sites. The number of rays in conducting phloem declined 1.4–2 times, whereas the ray fraction in both conducting and nonconducting phloem was 1.5–2 times higher than in typical habitats. Large areas of dilated parenchyma were formed, likely serving as local carbon and water reservoirs to mitigate crown damage and physiological drought. These results indicate deviations from reference ontogenetic trajectories of phloem rays under volcanic stress, suggesting structural adjustments that enhance radial transport and storage. Further integrative studies are needed to clarify how these modifications interact with xylem traits and contribute to whole-plant resilience.

Keywords: *Betula ermanii*, bark, ontogeny, conducting and nonconducting phloem, phloem rays, dilatation, volcanic environment, physiological drought

РЕЗЮМЕ

Копанина А.В., Тальских А.И., Власова И.И. Онтогенетические тренды в строении флоэмных лучей *Betula ermanii* (Betulaceae): адаптивные ответы на вулканическую активность. Выполнен сравнительный онтогенетический анализ (1–112 лет) флоэмной паренхимы внутренней коры *Betula ermanii* из ее типичных местообитаний на острове Сахалин и с термальных источников вулкана Баранского на острове Итуруп. Выявлено прямое положительное аллометрическое соотношение между жизненной формой и признаками радиальной системы флоэмы. Диаметр ствола увеличивался логарифмически с высокими коэффициентами детерминации, а возрастные тенденции признаков флоэмных лучей следовали логарифмическому паттерну в молодой коре (до 25–35 лет) и достигали плато в зрелой коре. В ходе онтогенеза общее число лучей уменьшилось в три раза, количество однорядных лучей сократилось в 6–9 раз, состав лучей изменялся начиная с 10-летнего возраста, а ширина лучей увеличивалась. В вулканической среде рост взрослых деревьев был замедлен по сравнению с типичными участками. Число лучей в проводящей флоэме уменьшилось в 1,4–2 раза, тогда как доля лучей как в проводящей, так и в непроводящей флоэме была в 1,5–2 раза выше, чем в типичных условиях. В условиях термальных источников в коре формировались большие участки дилатированной паренхимы, вероятно, служащие локальными резервуарами углерода и воды для компенсации повреждений кроны и физиологической засухи. Эти результаты указывают на отклонения от типичных онтогенетических траекторий флоэмных лучей под воздействием вулканического стресса, что свидетельствует о структурных адаптациях, повышающих эффективность радиального транспорта и хранения. Требуются дальнейшие комплексные исследования, которые позволят понять, как эти изменения взаимодействуют с признаками ксилемы и обеспечивают устойчивость растения в целом.

Ключевые слова: *Betula ermanii*, кора, онтогенез, проводящая и непроводящая флоэма, флоэмные лучи, дилатация, вулканический ландшафт, физиологическая засуха

Volcanic hydrothermal activity, including solfataras, fumaroles, thermal springs, streams, and lakes, has persisted for centuries, reshaping landscapes and generating habitats that are often stressful for plants (Manko & Sidelnikov 1989, Laverov et al. 2005). These systems supply juvenile pyroclastic material, hot mineralised waters, and aggressive gases into root-inhabited horizons, driving structural and floristic shifts in plant communities of Northeast Asia (Manko 1980, Grishin 2003, Neshataeva 2009, Korablev & Neshataeva 2016, Grishin et al. 2019, Neshataeva et al. 2021).

Conditions unique to hydrothermal zones include soils enriched with salts from major and trace metal ions but generally nutrient-poor; lower atmosphere layers saturated with toxic gases such as nitrogen and sulphur oxides, ha-

logen and sulphur hydrides; elevated soil temperatures; and acidic to ultra-acidic waters (Sokolov 1973, Gladkova & Butovets 1988, Manko & Sidelnikov 1989, Laverov et al. 2005, Goldfarb 2005, Zakharikhina & Litvinenko 2019).

Studies of vegetation in Kamchatka's hydrothermal fields show that substrate temperature, moisture gradients, soil acidity, and nutrient impoverishment are key factors controlling microzonation and stress intensity (Samkova 2009, Samkova et al. 2016, Korablev et al. 2018, Neshataeva et al. 2021, Korablev et al. 2024). However, structural analyses of woody plants in volcanic habitats remain scarce, and questions about their anatomical and functional adaptations to such extreme conditions are still unresolved.

Our recent studies indicate that woody plants growing in volcanic environments of the Kamchatka and Kuril Islands show distinctive adaptive structural features in both bark and wood (Eryomin & Kopanina 2012, Kopanina et al. 2017, Kopanina 2019, Kopanina & Vlasova 2019, Kopanina et al. 2020, Talskikh et al. 2022, Kopanina et al. 2022). Stress in these hydrothermal landscapes appears to induce physiological drought, thereby triggering adaptive structural responses in the carbon pathway (Kopanina et al. 2022).

The bark is a vital component of trees throughout their lifespan (Esau 1953, 1977, Evert 2006). The phloem, a complex conducting tissue, is central both to long-distance carbon transport and to storage of valuable metabolites. Its functions rely on intricate structural connections between sieve-tube and parenchyma and undergo substantial age-related transformations during ontogeny (Esau 1953, 1977, Gamalei 2004, Evert 2006, De Schepper et al. 2013, Liesche et al. 2016, Savage et al. 2017, Holbrook & Knoblauch 2018, Furze et al. 2018, Clerx et al. 2020, Van Bel 2021).

Trees have therefore evolved complex mechanisms enabling the bark to adjust metabolism and transport processes under stress, including low temperatures (Molina 2016, Lintunen et al. 2016, Schröter & Oberhuber 2021) and drought (Lintunen et al. 2016, Sevanto 2018, Levionnois et al. 2021, McCubbin & Braun 2021).

Recent researches have shown that phloem parenchyma retains water during drought, preventing its backflow into the xylem along concentration gradients (Pfautsch et al. 2015, Huang et al. 2018, Sevanto 2018, Inagawa et al. 2023). Although theories on drought impacts on plant water transport are well established, the specific effects on phloem transport have only recently attracted significant attention (Sevanto 2018). Studies of mechanisms supporting phloem transport emphasise the role of phloem parenchyma in redistributing water and carbon, both in the main long-distance pathway and in radial (short-distance) transport (Thompson 2006, Hölttä et al. 2009, De Schepper et al. 2013, Sellier & Harrington 2014, Pfautsch et al. 2015).

Few studies have addressed structural changes in ray fraction and phloem parenchyma during tree growth, i.e. with increasing stem diameter, age, and height (Esau 1965, Khan et al. 1981, Eryomin 1982, 1983, Lev-Yadun & Aloni 1990, Trockenbrodt 1991, Petit & Crivellaro 2014, Woodruff 2014, Jyske & Hölttä 2015, Savage et al. 2017, Liesche & Schulz 2018, Clerx et al. 2020). Even fewer studies have considered the ecological significance of phloem traits during ontogeny (Tarelkina et al. 2024), including our own (Kopanina & Vlasova 2019, Kopanina et al. 2022). Structural and functional relationships among phloem elements within the highly variable and multifunctional bark of woody plants (Rosell et al. 2014, Shtein et al. 2023) remain far from fully understood but represent a promising area of bark functional ecology (Rosell et al. 2014, Schröter & Oberhuber 2021, Shtein et al. 2023, Gričar 2024).

Betula ermanii Cham. (Betulaceae), commonly known as stone birch, is widespread across Northeast Asia, including diverse volcanic landscapes, where it forms distinct Far Eastern forest formations. We have studied *B. ermanii* in various environments on Sakhalin and in the southern Kuril Islands, and found that its carbon transport pathway shows structural–functional adaptations under natural stress, particularly in volcanic habitats (Talskikh et al. 2022, Kopanina et al. 2022). Structural responses to thermal springs and mud-volcanic breccias were reflected in variation of sieve-tube elements, associated with enhanced conductivity and increased carbon resource availability for growth (Kopanina et al. 2022). Nevertheless, structural and functional relationships among phloem elements remain incompletely understood, and the architecture of the whole bark tissue complex, especially under high salinity of volcanic substrates, is still poorly documented.

In this study, we examine ontogenetic structural patterns of phloem parenchyma in the bark of *B. ermanii* from thermal spring habitats of Baransky Volcano (45.103°N 148.016°E, Iturup Island) and from typical forest stands in southern Sakhalin. We hypothesise that volcanic stress, which is associated with elongation and expansion of sieve-tube elements (Kopanina 2019, Kopanina & Vlasova 2019, Kopanina et al. 2022), also promotes an increase in the volume of phloem parenchyma, particularly rays, thereby optimising both long-distance and radial transport pathways.

We focused specifically on ray parenchyma under the influence of the stressful volcanic environment, as it is the most variable tissue in response to environmental factors compared with diffuse parenchyma in the phloem and apotracheal axial parenchyma in the xylem, both characteristic of *B. ermanii*. A global comparative analysis of more than 2,000 woody angiosperm species by Morris et al. (2018) showed that in species with apotracheal parenchyma there is no statistically significant relationship with xylem vessel conductivity efficiency across contrasting environments.

MATERIAL AND METHODS

The interpretation of *B. ermanii* in this study follows the latest taxonomic revision of the genus *Betula* L. (Ashburner & McAllister 2016). *Betula ermanii* is a polytypic species, and its populations are highly polymorphic (Shemberg 1986, Nedoluzhko & Skvortsov 1996). The species occupies a wide area of the Russian Far East, from 39 to 61°N and from 108 to 164°E, including Honshu, Hokkaido, Sakhalin, and many of the Kuril Islands (Ohwi 1965, Skvortsov et al. 1977, Miyawaki 1985, Shemberg 1986, Li & Skvortsov 1999, Barkalov 2009). Its ecological niche is associated with mountain habitats in the cold marine climate of the northern Pacific (Shemberg 1986, Krestov 2003). Trees reach 20–25 m in height, with stem diameters of 50–75 cm (occasionally up to 90 cm), and may live for 250 years.

Two contrasting sites of *B. ermanii* were selected: (1) a typical forest environment beyond volcanic influence in the East Sakhalin Mountains (site T1 and T2, Table 1, Fig. 1A–E), and (2) habitats near the hot springs of Baransky Volcano in the Grozny Range on Iturup Island (site VA, Table 1, Fig. 1F–H). The reference sites, unaffected by volcanism, were Krasnaya Mt. (site T1) (Fig. 1A, B) and Bolshevik Mt. (site T2) (Fig. 1C–E), both situated within the Susunai Range and its foothills. As trees at Krasnaya Mt were no older than 69 years, we additionally sampled 112-year-old trees from the ecologically similar Bolshevik Mt. site (Table 1). Samples were collected during the growing seasons of 2015–2020, from mid-September to late October, during the defoliation period.

At the Baransky Volcano (site VA), specimens of *B. ermanii* were collected along the shores of the Golubye Ozera thermal springs (Table 1, Fig. 1F). Baransky Volcano (also known as Baranskii, Iiusu, Sashiusu, Sashiusudake) is an active stratovolcano (1132 m a.s.l.) with persistent fumarolic activity from the summit and several flank craters; the geothermal field includes hot springs and geysers (Gorshkov 1967, McClelland 1992, VOKKIA IVS FEB RAS). The Golubye Ozera thermal springs, located in the middle course of the Kipyashchaya River, consist of two funnels filled with sulphate–chloride water, where SO_4^{2-} concentrations reach 2381 $mg \cdot L^{-1}$. The water is ultra-acidic (pH 1.2) and hot, with temperatures up to 107.5°C. Sulphur is dispersed along the shores, and CO_2 (38.2 % vol.) is the dominant gas (Zharkov 2014, Bragin et al. 2019).

At each of the three sites, trunk diameters (at 0.5 m and 1.3 m) and tree height were measured for 15 individuals. Three model *B. ermanii* trees were selected (Table 1). Trees were felled with a chainsaw approximately 50 cm above ground and sectioned into 7–10 cm discs at 1–2 m intervals along the stem. From each disc and from branches at different developmental stages, blocks of 5–10 cm were taken for anatomical analysis. Crown samples were represented by one large sun-exposed branch to avoid shading effects. Additionally, twigs and branches of different ages representing all stages of bark transformation were collected from each model tree. Ages and stem diameters were determined (Tables 1, 2) by counting growth rings under a LOMO stereomicroscope (Russia) in the laboratory. Samples were fixed on the day of collection in a mixture of 50 % ethanol and glycerol (3:1), and then stored in 70 % ethanol and glycerol (3:1) for at least two months before sectioning. Herbarium vouchers were deposited in the Institute of Marine Geology and Geophysics FEB RAS (IMGG FEB RAS), Yuzhno-Sakhalinsk, Russia (SAK). Wood and bark samples were deposited in the Plant Ecology Laboratory of IMGG FEB RAS.

From each trunk disc and branch, bark fragments or whole stem pieces (0.5–2 cm) were cut for laboratory examination. All samples were incubated in distilled water for 12–72 h, depending on bark age, to remove fixing fluids. Transverse, radial, and tangential sections (10–25 μm thick) were prepared with a sledge microtome HM 430c equipped with a fast-freeze device (Thermo Scientific, USA). Sections from fixed material were stained with a mixture of safranin and Nile blue (Prozina 1960, Barykina et al. 2004) and washed in a graded ethanol series (up to 96 %) for dehydration. Final dehydration was carried out in carbol xylol and xylol, after which the samples were embedded in a xylene-based mounting medium (Cytoseal-60, Thermo Fisher Scientific, USA). For each site, 370–460 permanent slides were prepared. Sections were studied using a light microscope Axio Scope. A1 (Carl Zeiss, Germany) and ZEN 2 software (Carl Zeiss, Germany). Descriptive terminology follows the IAWA List of Microscopic Bark Features (Angyalossy et al. 2016).

To compare quantitative data of bark traits, which undergo profound structural changes with increasing stem age and diameter, we adopted the following study design. Traits were measured in two bark zones: the conducting phloem adjacent to the vascular cambium, and the dilated nonconducting phloem located next to it. The latter zone was delimited at the bark periphery by the boundary of a massive

Table 1. Key sites and model trees of *Betula ermanii* in the Susunai Range (Sakhalin Island) and at Baransky Volcano (Iturup Island, Kuril Archopelago).

Study site	**Krasnaya Mt. (Sakhalin Isl.) not affected by volcanism**	**Bolshevik Mt. (Sakhalin Isl.) not affected by volcanism**	**Golubye Ozera (Iturup Isl.) affected by volcanism**
Study site code	**Site T1**	**Site T2**	**Site VA**
Coordinates	46.935°N 142.838°E	46.953°N 142.791°E	44.980°N 147.820°E
Elevation of sample collection (m a.s.l.)	574	284	251
Plant community	Stone-birch-fir (*Betula ermanii* and *Abies sachalinensis*) forest with shrubs and herbs	Stone-birch (*Betula ermanii)* forest with shrubs and tall herbs	Sparse *Betula ermanii*, *Larix kurilensis* and *Sasa kurilensis* forest
Life form	Single-stemmed tree	Single-stemmed tree	Single-stemmed tree
Stem age (yr)	50, 54, 60	103, 111, 112	63, 73, 73
Axial height (m)	15, 15.5, 17	21, 21, 24	4, 4.6, 5
Trunk diameter at 1.3 m/0.5 m height (cm)	16.3, 18.6, 20.5/21.4, 23.5, 26	34.4, 55, 55.4/39.5, 61, 59.3	10, 12, 12.2/13.9, 14.4, 15
Rhytidome	Present at trunk base	Present up to two meters along the trunk	Present
Crown damage score (1–10)	1	1	5
Heat and gas burns on leaves and stems	none	none	present
Bark sample age (ring number) (yr)	1, 2, 3, 4, 5, 6, 7, 9, 10, 13, 23, 30, 35, 50, 54, 63, 69	103, 111, 112	1, 2, 3, 4, 5, 6, 8, 9, 10, 12, 14, 17, 23, 26, 42, 56, 63, 73

Figure 1 Sampling sites of *Betula ermanii* Cham. in southern Sakhalin and Iturup Islands (field photographs): A, B – typical forest site – site T1, Krasnaya Mt., Susunai Range, Sakhalin Island, 25.10.2020; A – tree; B – main stem (trunk) with rhytidome; C, D, E – typical forest site – site T2, Bolshevik Mt., Susunai Range, Sakhalin Island; C – tree, 20.10.2019; D – main stem (trunk) with rhytidome, 05.07.2020; E – 2-yr old twigs, 23.06.2019; F, G, H – Golubye Ozera thermal springs – site VA, Baransky Volcano, Grozny Range, Iturup Island, 27.07.2018; F – tree; G – main stem (trunk) with periderm; H – 2-yr old twigs

Table 2. Stem diameter variation of *Betula ermanii* with age in the Susunai Range (Sakhalin Island, sites T1 and T2) and at Baransky Volcano (Iturup Island, site VA). Data are presented as sample mean (SM) ± confidence interval (CI); values in braces are 5th and 95th percentiles; numbers below show sample size (SS). Ages in brackets refer to the volcanic site. Bolshevik Mt. data correspond to ages 85 and 112.

Stem age (yr)	Typical sites (T1 and T2)	Volcanic site (VA)
1	2.20 ± 0.07 (1.86-2.49) 36	2.38 ± 0.15 (2.00-2.81) 32
2	3.44 ± 0.21 (2.84-4.90) 45	4.75 ± 0.37 (2.50-7.30) 57
3	5.33 ± 0.27 (4.01-7.00) 42	6.18 ± 0.32 (5.10-8.12) 38
4	7.04 ± 0.32 (6.00-8.62) 33	8.29 ± 0.74 (6.00-11.5) 24
5	7.80 ± 0.44 (6.08-9.00) 26	11.6 ± 0.88 (9.21-15.2) 23
6	13.3 ± 1.26 (7.63-18.2) 26	11.3 ± 0.76 (8.43-14.9) 26
7(8)	11.6 ± 1.05 (7.39-15.0) 30	17.8 ± 1.53 (10.1-15.2) 25
9	15.9 ± 1.04 (12.5-19.9) 27	18.6 ± 1.86 (11.8-22.9) 24
10	19.3 ± 1.37 (15.0-24.0) 22	24.3 ± 1.82 (16.8-31.9) 30
13(12)	29.9 ± 2.18 (17.5-35.6) 30	30.3 ± 2.55 (16.2-41.0) 31
23(14)	50.5 ± 4.74 (38.4-73.7) 28	38.2 ± 4.58 (27.3-60.5) 31
30(17)	68.8 ± 2.28 (61.7-74.0) 18	45.1 ± 4.55 (24.7-55.8) 28
35(23)	81.1 ± 3.58 (70.7-87.0) 15	63.9 ± 8.17 (41.8-95.6) 30
54(26)	168.1 ± 5.72 (159.3-189.1) 15	74.4 ± 7.11 (60.4-94.3) 15
63(42)	181.9 ± 8.77 (160.0-200.0) 15	102.1 ± 5.23 (90.7-115.6) 15
69(56)	226.0 ± 8.35 (205.0-243.6) 15	128.9 ± 5.00 (116.2-140.3) 15
85(63)	318.2 ± 15.9 (271.7-346.7) 15	137.0 ± 5.23 (124.4-155.9) 15
112(73)	550.9 ±22.7 (507.1-592.6) 15	148.9 ± 6.07 (139.0-165.0) 15

sclerified nonconducting phloem. This approach allowed us to avoid distortion of quantitative data caused by strong dilatation and the activity of sequent periderms during rhytidome formation at the mature bark periphery in *B. ermanii*.

We analysed *B. ermanii* bark samples from trees of different ages and stem diameters (Table 2). This research design followed the methodological recommendations of von Arx et al. (2015), developed for ecological studies of xylem ray parenchyma. These authors emphasise the strong intrinsic and allometric components of ray variability compared with the weaker environmental signal. We therefore considered it necessary, in order to identify ecological responses in the structure of phloem rays, to analyse their variation in relation to stem diameter and age at different tree heights across habitats. In transverse sections, the traits listed in Table 3 were measured according to the methods of Yatsenko-Khmelevsky (1954), von Arx et al. (2015), and Angyalossy et al. (2016): width of conducting and nonconducting phloem; in conducting phloem total number of rays per mm, number of uniseriate rays per mm, number of rays > 4-seriate per mm, ray width in conducting phloem (cells per ray), ray / sieve-tube fraction, %; and ray / sieve-tube fraction in nonconducting phloem, %.

Measurement data (sample size) for each anatomical trait were combined across each site and for all three model trees. Thus, for each character one parameter based on 15–32(112) measurements was obtained for statistical analysis. For each age range and site (Tables 2, 3) we analysed stem diameters, tissue, and cell characters to calculate the sample mean (SM) and its 95 % confidence interval (CI) using Student's t-distribution. Non-overlapping CIs were considered to indicate significant differences between SM. This approach is essentially equivalent to Student's t-test for comparing mean values of two samples. We therefore compared the SM of each trait at volcanic and typical sites within the same age class.

Least-squares regression analysis was used to examine age trends (patterns of variation in bark traits with age and stem diameter) at volcanic and reference sites. Regression equations and coefficients of determination (R^2) were reported for each trend. These age-related trends allowed us to assess the rate and direction of change in bark traits, given the different ages and diameters of trees at each site. Statistical analyses were performed using R version 4.2.0 (R Core Team, 2022) and Microsoft Excel.

RESULTS

Stem diameter–age trends and rhytidome initiation

We analysed variations in stem diameter with age in *B. ermanii* trees from typical environments on Sakhalin Island and from the thermal springs of Baransky Volcano, Iturup Island (Tables 1, 2; Fig. 2). Age and stem diameter (in both twigs, branches and trunks) exhibit an almost linear relationship in logarithmic coordinates, as demonstrated by analyses based on the entire dataset (Fig. 2). The curvature of this relationship is slight but differs in sign between habitats: it is positive (0.204) under typical conditions and negative (-0.001) under volcanic ones (Fig. 2). Notably, the pronounced divergence of the curves describing the relationship between age and stem diameter at older ages may reflect more favourable light conditions for trees at site T2. The correlation between age and stem diameter is very strong, with coefficients of determination exceeding $R^2 = 0.96$ across all sites (Fig. 2).

Up to 25–30 years, the diameters of branches and young trunks at the site VA were slightly larger and their increase with age was faster than at the typical site (Table 2;. Fig. 2).

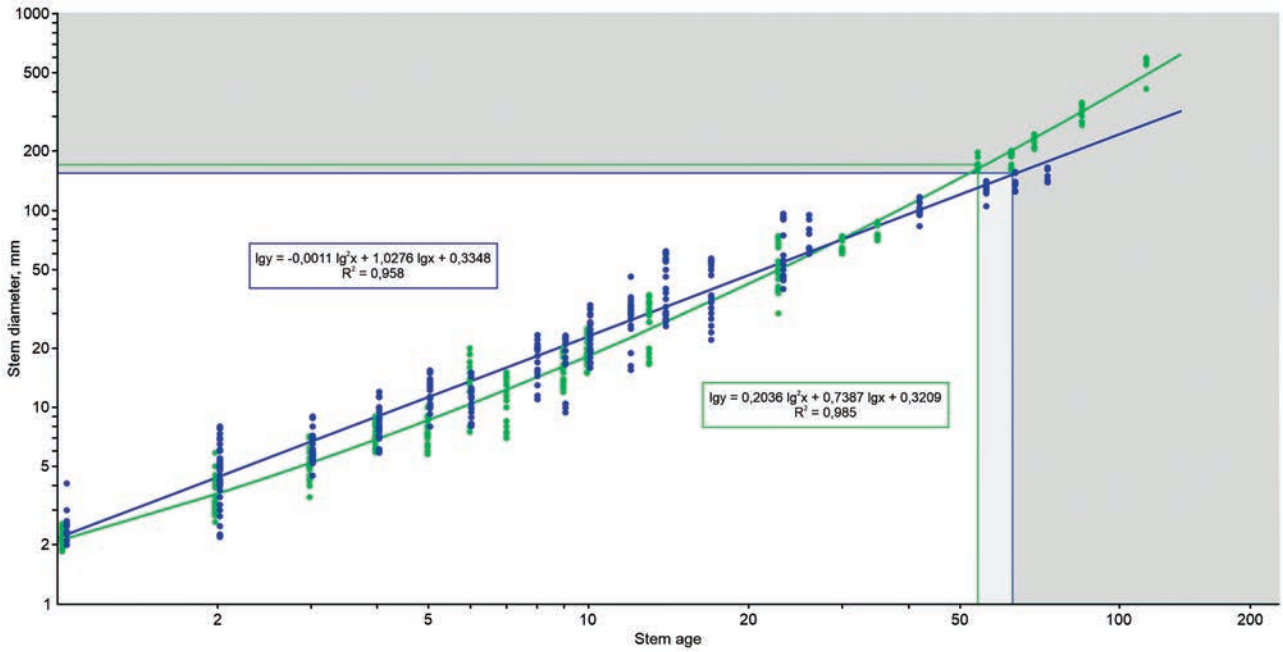

Figure 2 Log-linear regression of stem diameters on age in Betula ermanii Cham.: green line and points are typical sites (T1 and T2) on Krasnaya & Bolshevik Mts, Susunai Range, Sakhalin Island; blue line and points are the site VA on Baransky Volcano, Grozny Range, Iturup Island; regression equations and coefficients of determination (R^2) are shown in boxes

After 25–30 years an inversion occurred: mature trunks were significantly smaller and their increase with age was slower than at the typical site (Fig. 2). Based on the logarithmic trend, we can expect that at 100 years trunks at the site VA will reach about 230 cm in diameter, whereas at the typical site they will be 1.8 times larger (409 cm) (Fig. 2).

The trends also indicate that rhytidome formation in *B. ermanii* depends on both age and stem diameter (Fig. 2). At the typical site, rhytidome was first observed on stems of 54-year-old trees, whereas in the volcanic environment it appeared at about 63 years. At this age, stem diameter at the typical site was 1.2 times larger (Table 2; Fig. 2). Rhytidome occupied extensive areas of bark trunks at the site VA from 73 years of age with an average diameter of 149 mm, and at the typical site from 69 years with an average diameter of 226 mm (a 1.5-fold increase) (Table 2; Fig. 2). Thus, rhytidome initiation occurred at similar ages and trunk diameters in both environments, while its extensive development occurred at comparable ages but with smaller trunk diameters at the volcanic site.

Ontogenetic changes in phloem ray of crown twigs and branches

The bark structure, phloem rays, and axial parenchyma of *B. ermanii* were described in our previous work (Kopanina et al. 2022). In 1-year-old bark, the outer layer consisted of the first periderm (Fig. 3A,B). The diameters of 1-year-old twigs were close in both habitats, allowing direct comparison of phloem structure (Tables 2, 3; Figs 2, 4, 5). All secondary phloem rays were direct extensions of xylem rays, retaining the same orientation (Fig. 3C, D). Rays contained procumbent, square, and upright cells intermixed throughout, with an average height of about 300 µm. By the end of the growing season, ray cells in the early secondary phloem became dilated due to growth (Fig. 3E,F). At the site T1, the total number of rays in 1-year-old bark was 27–28 per mm, with most being uniseriate (25–26 per mm) (Table 3; Fig. 4A–D). Occasional 2–3-seriate and rarely 4-seriate rays were also present. At the site VA, the number of both uniseriate and multiseriate rays was significantly lower (23–25 per mm) compared to the typical site (Table 3; Fig. 4A–D). The axial parenchyma was diffuse and showed no distinctive features in the volcanic environment (Fig. 3E,F).

The ring zone of nonconducting phloem first appeared in 2-year-old bark (Fig. 6C–F). Twigs diameters in 2-year-old did not differ substantially between sites (Tables 2, 3; Figs 2, 4, 5). At the site T1, the widths of conducting and nonconducting phloem were equal (40 µm), whereas at the site VA they measured 50 µm and 34 µm, respectively (Table 3; Fig. 6C,D). Rays in both zones expanded through cell enlargement (Fig. 6E,F). Some rays exhibited pronounced cell dilatation, while in others the cells did not expand (Fig. 6E,F). Cortex–phloem contact was maintained by parenchyma cells between sclereids and protophloem fibres (Fig. 6C,D). The total number of conducting phloem rays decreased by ~60 % compared with 1-year-old bark: 18–20 rays per mm at the site T1 and 18–19 per mm at the site VA (Table 3; Fig. 4A,D). This reduction was mainly due to the loss of uniseriate rays (Table 3; Fig. 4C,D). Ray widths in conducting phloem were similar across sites (Table 3; Fig. 4E,F). The axial parenchyma remained diffuse and featureless in the volcanic habitat (Fig. 6E, F).

In 5-year-old bark, the surface consisted of peeling phellem layers formed by the first periderm (Fig. 7A,B). The twigs diameters at the site VA were slightly larger compared with those at the typical site (Tables 2, 3; Figs 2, 4, 5). At the site T1, nonconducting phloem was already three times wider than conducting phloem, and at the site VA 5.5 times wider (Table

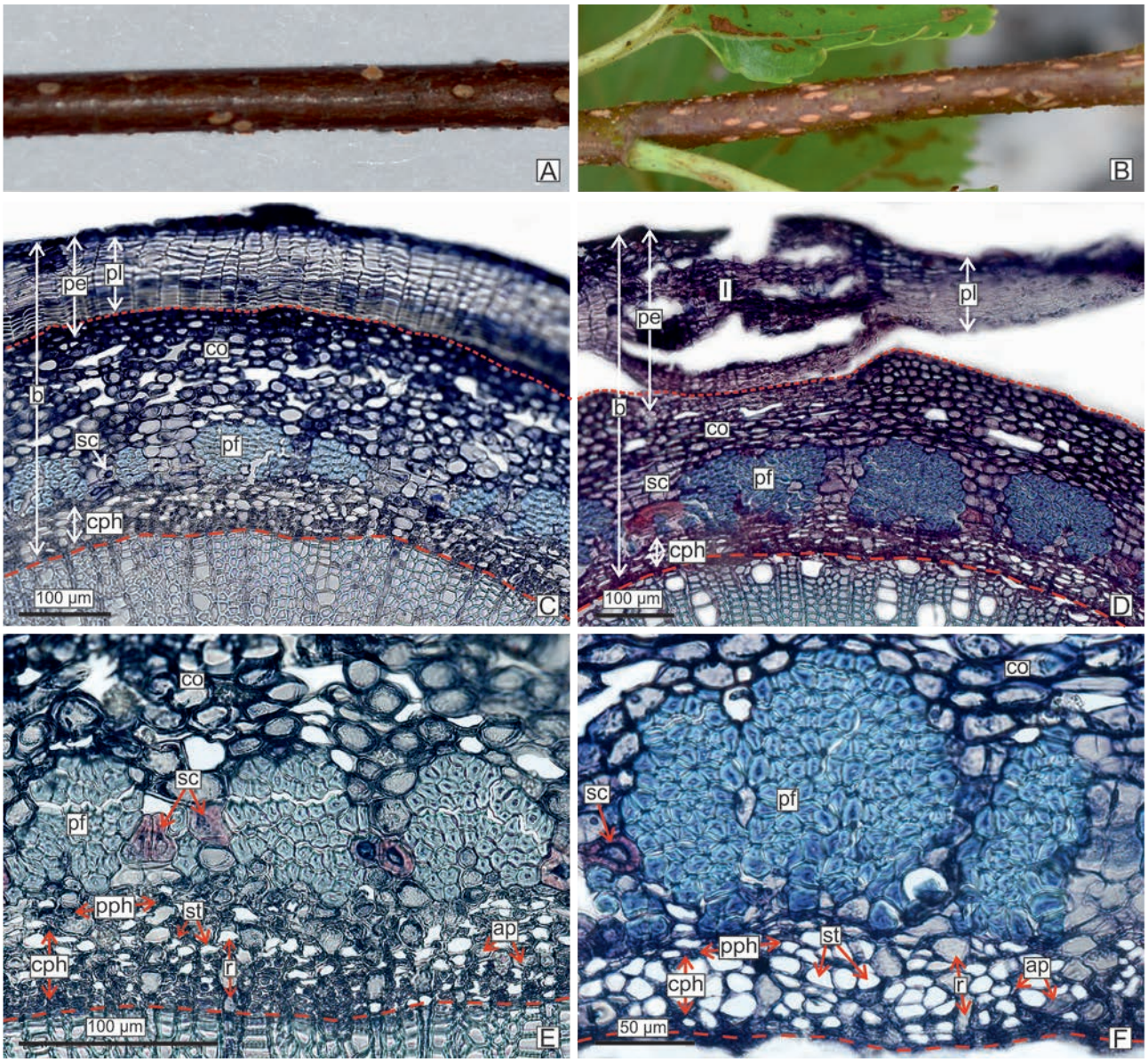

Figure 3 Bark of 1-yr old stems of *Betula ermanii* Cham. from southern Sakhalin and Iturup (site VA) Islands: A, C, E – site T1; B, D, F – (site VA); A, B – outer surface of stem bark; C, D – bark; E, F – inner bark zone; transverse section; red small dotted line is a phellogen; red dotted line is a vascular cambium. Abbreviations, stand for names of bark tissues: axial parenchyma (ap), bark (b), cortex (co), conducting phloem (cph), dilated ray (dr), dilatated nonconducting phloem (dnph), sclereids group (gsc), lenticel (l), nonconducting phloem (nph), periderm (pe), primary phloem (pph), protophloem fibers (pf), phellem (pl), ray (r), pseudocortex (pco), rhytidome (rh), sclereids (sc), sclerified nonconducting phloem (snph), sieve-tube element (st)

3; Fig. 7C,D). Phloem parenchyma dilated as rays expanded, with some rays forming wedge-shaped structures in the nonconducting phloem (Fig. 7C,D). Expansion occurred through both cell growth and cell division. A continuous sclerenchyma ring developed from protophloem fibres and brachysclereids derived from rays and axial parenchyma (Fig. 7C,D). The total number of rays in conducting phloem continued to decline (Table 3; Fig. 4A,D). The vascular cambium progressively ceased producing uniseriate and biseriate rays, while still generating multiseriate rays, both towards phloem and xylem (Table 3; Fig. 4E,F). Uniseriate rays, however, remained predominant. In typical sites, 13–14 out of 15 rays per mm were uniseriate (Table 3; Fig. 4A,D), whereas at the site VA only 5–7 out of 11 rays per mm were uniseriate. Ray width at the site VA increased to 2.6–3 cells on average (Table 3; Figs 4E,F, 7). Ray and sieve-tube fraction in conducting phloem was similar across sites (20–21 % and 64–66 %, respectively; Table 3; Fig. 5A,D). Comparable values were found in the nonconducting phloem (23–27 % and 58–60 %; Table 3; Fig. 5E–H). Axial parenchyma was diffuse and featureless in the volcanic site (Fig. 7E,F).

By 10 years, nonconducting phloem accounted for nearly half of total bark width (Table 3; Fig. 8C,D). The difference in branch diameters between 5 and 10 years persisted between the volcanic and typical habitats (Tables 2, 3; Fig. 2). Stem diameters at the site VA were 1.2–1.5 times larger (Table 2; Fig. 2). Ray dilatation dominated in nonconducting phloem, with wedge-shaped rays regularly present in its outer layers (Fig. 8C,D). Sclereid groups appeared in the outer nonconducting phloem, contacting the sclerenchyma

Table 3. Phloem traits of *Betula ermanii* in the study sites T1 and T2 on Susunai Range, Sakhalin Island and in the study site VA on Baransky Volcano, Iturup Island

Stem age (yr)	Phloem traits																			
	Nonconducting phloem width, µm		Conducting phloem width, µm		Total number of rays in conducting phloem per mm		Number of uniseriate rays in conducting phloem per mm		Number of rays > 4-seriate in conducting phloem per mm		Ray width in conducting phloem (cells per ray)		Ray fraction in conducting phloem, %		Sieve-tube fraction in conducting phloem, %		Ray fraction in nonconducting phloem (inner bark), %		Sieve-tube fraction in nonconducting phloem (inner bark), %	
	Sites T1+T2	Site VA	Sites T1+T2	Site VA	Sites T1+T2	Site VA	Sites T1+T2	Site VA	Sites T1+T2	Site VA	Sites T1+T2	Site VA	Sites T1+T2	Site VA	Sites T1+T2	Site VA	Sites T1+T2	Site VA	Sites T1+T2	Site VA
1	–	–	41.4 ± 1.24 (32.1-50.9) 96	45.0 ± 2.75 (35.9-61.8) 32	27.1 ± 0.49 (23.0-31.0) 112	23.9 ± 0.82 (20.6-27.0) 32	25.9 ± 0.50 (22.0-30.0) 112	23.7 ± 0.85 (20.0-27.0) 32	0 – 112	0 – 32	2.05 ± 0.13 (1.00-3.00) 112	1.22 ± 0.15 (1.00-2.00) 32	–	–	–	–	–	–	–	–
2	39.2 ± 2.19 (25.2-54.3) 64	33.6 ± 2.13 (26.6-41.6) 32	37.6 ± 1.74 (26.0-50.8) 64	49.0 ± 2.63 (38.5-61.2) 32	19.5 ± 0.38 (17.0-22.0) 64	18.8 ± 0.65 (16.0-21.5) 32	18.3 ± 0.49 (16.0-21.0) 64	18.3 ± 0.60 (16.0-21.0) 32	0 – 64	0 – 32	1.73 ± 0.34 (1.00-3.00) 64	1.47 ± 0.20 (1.00-2.00) 32	–	–	–	–	–	–	–	–
5–8	150.7 ± 4.84 (130.6-169.5) 32	271.7 ± 18.6 (204.2-343.5) 32	43.4 ± 2.58 (33.7-55.3) 32	47.6 ± 2.45 (39.1-59.5) 32	15.0 ± 0.37 (14.0-17.0) 32	11.0 ± 0.44 (9.00-13.0) 32	13.9 ± 0.48 (12.0-16.5) 32	6.25 ± 0.53 (4.00-8.00) 32	0 – 32	0 – 32	1.81 ± 0.23 (1.00-3.00) 32	2.81 ± 0.21 (2.00-4.00) 32	20.1 ± 1.01 (15.5-24.4) 32	20.7 ± 0.75 (17.7-23.9) 32	65.7 ± 1.41 (58.3-70.3) 32	67.1 ± 1.67 (58.9-73.9) 32	24.6 ± 1.22 (19.0-31.4) 32	26.9± 1.22 (22.6-33.5) 32	59.2 ± 1.89 (49.5-67.5) 32	59.7 ± 1.94 (51.4-65.9) 32
10–14	572.6 ± 15.6 (508.1-634.5) 32	613.4 ± 18.5 (541.4-685.0) 32	100.3 ± 4.45 (85.8-119.1) 32	83.0 ± 2.95 (71.1-96.6) 32	13.2 ± 0.54 (11.0-15.5) 32	11.9 ± 0.55 (9.55-14.5) 32	8.72 ± 0.63 (6.00-11.0) 32	7.69 ± 0.58 (5.00-10.0) 32	0.03 ± 0.06 (0.00-0.00) 32	0.16 ± 0.16 (0.00-1.00) 32	2.72 ± 0.19 (2.00-3.00) 32	3.03 ± 0.19 (2.55-4.00) 32	20.9 ± 1.15 (16.8-25.8) 32	21.9 ± 1.08 (17.2-25.9) 32	68.0 ± 1.48 (59.8-74.1) 32	67.4 ± 1.71 (60.8-74.3) 32	26.9 ± 1.70 (21.1-33.1) 32	31.0 ± 1.64 (23.7-39.3) 32	61.6 ± 2.17 (52.9-68.0) 32	56.1 ± 1.71 (49.0-63.5) 32
21–24	1067.8 ± 36.4 (881.6-1226.8) 42	1432.4 ± 34.3 (1245.5-1548.3) 32	102.2 ± 3.51 (83.7-121.5) 42	117.6 ± 4.66 (99.4-134.3) 32	11.0 ± 0.42 (9.00-13.0) 32	8.50 ± 0.48 (7.00-11.0) 32	6.34 ± 0.51 (5.00-8.45) 32	4.63 ± 0.46 (3.00-7.00) 32	0.06 ± 0.09 (0.00-0.45) 32	0.09 ± 0.11 (0.00-1.00) 32	2.91 ± 0.17 (2.00-3.45) 32	3.09 ± 0.11 (3.00-4.00) 32	16.1 ± 1.09 (11.6-21.1) 32	13.7 ± 0.96 (9.37-17.7) 32	76.6 ± 1.18 (71.2-81.3) 32	80.5 ± 1.24 (75.0-84.9) 32	18.4 ± 1.29 (13.7-25.2) 32	24.3 ± 1.82 (17.1-30.8) 32	73.5 ± 1.76 (66.9-80.5) 32	67.1 ± 2.03 (60.8-75.9) 32
54–56	3669.5 ± 139.2 (3095.5-4422.7) 44	1387.9 ± 31.7 (1264.3-1521.5) 32	107.0 ± 3.08 (81.6-132.9) 105	106.6 ± 2.51 (92.1-124.6) 64	8.64 ± 0.35 (7.35-10.0) 28	8.38 ± 0.42 (7.00-10.0) 32	4.39 ± 0.40 (3.00-6.00) 28	4.31 ± 0.40 (3.00-6.45) 32	0.64 ± 0.26 (0.00-2.00) 28	0.03 ± 0.06 (0.00-0.00) 32	3.57 ± 0.22 (3.00-4.00) 28	3.03 ± 0.06 (3.00-3.00) 32	15.7 ± 0.96 (11.9-20.0) 32	18.8 ± 1.67 (10.8-26.0) 32	77.0 ± 1.23 (72.5-84.9) 32	76.2 ± 1.62 (68.3-82.1) 32	22.6 ± 1.58 (15.4-28.5) 32	28.2 ± 1.66 (21.6-35.4) 32	68.8 ± 1.91 (60.8-77.4) 32	62.7 ± 1.77 (55.6-68.7) 32
73	–	1728.1 ± 92.2 (1374.7-2092.9) 45	–	110.8 ± 4.00 (93.1-130.0) 45	–	8.48 ± 0.37 (7.00-10.0) 33	–	2.55 ± 0.36 (1.00-4.00) 33	–	0.27 ± 0.16 (0.00-0.00) 33	–	3.27 ± 0.16 (3.00-4.00) 33	–	22.1 ± 1.21 (17.2-29.1) 32	–	70.4 ± 1.98 (59.3-77.3) 32	–	40.3 ± 1.93 (33.4-50.4) 32	–	50.2 ± 2.04 (39.1-57.5) 32
103	4354.6 ± 62.1 (3963.5-4560.5) 32	–	148.7 ± 5.20 (127.5-173.8) 35	–	9.28 ± 0.43 (8.00-11.0) 32	–	4.50 ± 0.39 (3.00-6.00) 32	–	0.41 ± 0.22 (0.00-1.45) 32	–	3.34 ± 0.17 (3.00-4.00) 32	–	–	–	–	–	–	–	–	–
112	5223.6 ± 191.6 (4702.7-6270.3) 25	–	140.3 ± 6.12 (112.5-168.4) 35	–	8.63 ± 0.43 (7.00-10.5) 32	–	4.16 ± 0.38 (3.00-6.00) 32	–	0.19 ± 0.17 (0.00-1.00) 32	–	3.22 ± 0.18 (3.00-4.00) 32	–	14.3 ± 0.89 (10.4-18.0) 32	–	81.5 ± 1.22 (75.6-87.2) 32	–	23.2 ± 1.40 (16.2-29.8) 32	–	69.0 ± 1.69 (63.3-76.1) 32	–

Note: Values of nonconducting phloem width, conducting phloem width, total number of rays in conducting phloem per mm, and number of uniseriate rays in conducting phloem per mm at ages 1, 2, 5–8, 10–14, 21–24, and 54–56 years are from Kopanina et al. (2022). Data are presented as sample mean (SM) ± confidence interval (CI); values in braces are 5th and 95th percentiles; numbers below show sample size (SS). Bolshevik Mt. data correspond to ages 103 and 112.

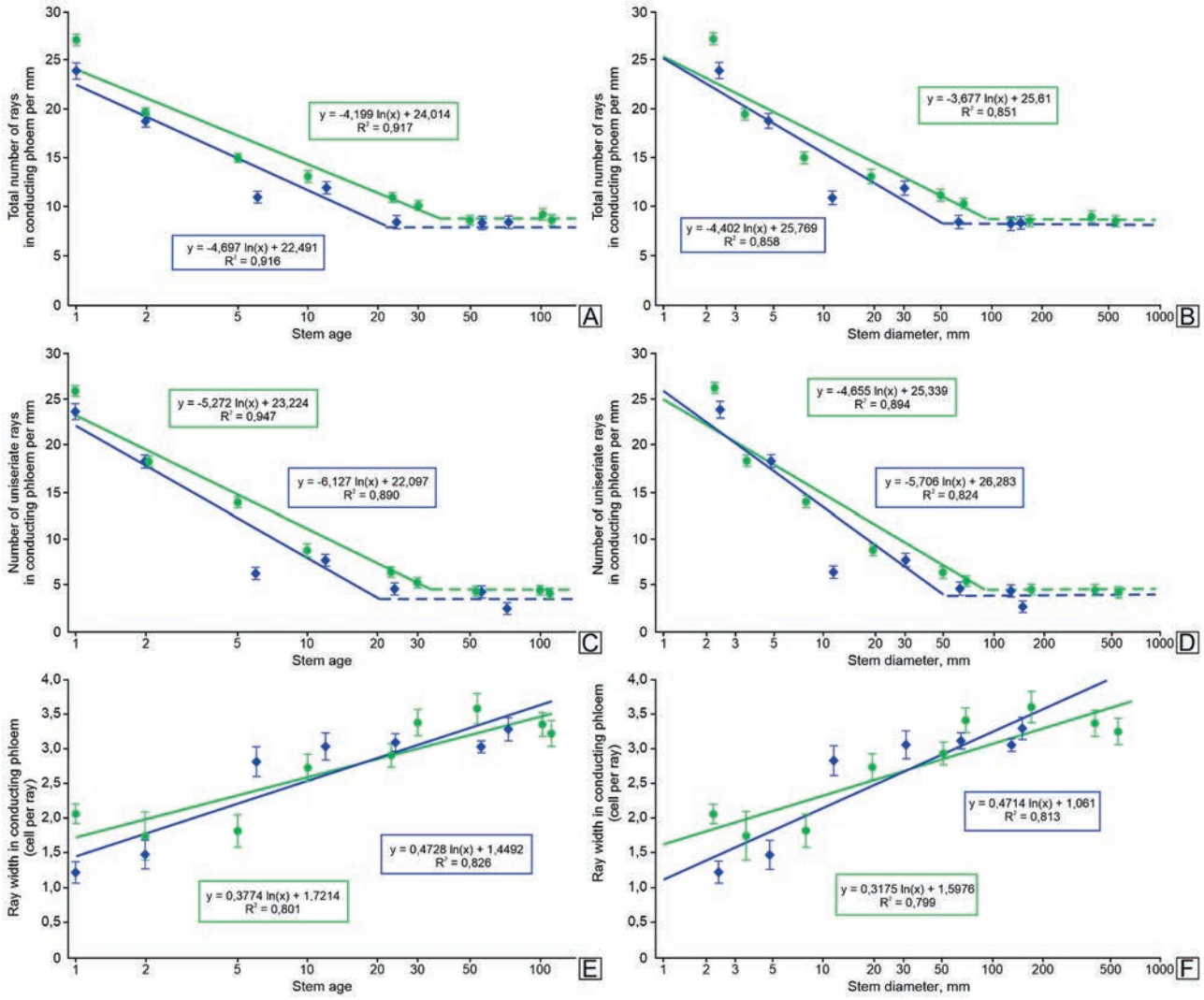

Figure 4 Relationships between phloem ray traits in the conducting phloem and tree age and stem diameter of *Betula ermanii* Cham. from southern Sakhalin and Iturup Islands: A, B – total number of rays per mm; C, D – number of uniseriate rays per mm; E, F – ray width (cells per ray); green lines are typical sites (T1 and T2) on Krasnaya & Bolshevik Mts, Susunai Range, Sakhalin Island; blue lines are the site VA on Baransky Volcano, Grozny Range, Iturup Island; log-linear regression for solid lines & schematic timeline for dotted lines; error bars show confidence interval (CI); regression equations and coefficient of determination (R^2) are given in boxes. The proportion of variance explained by this relationship below 0.67 is indicated by dotted lines (green and blue)

ring formed earlier (Figs 7C,D; 8C,D). These groups contained sclerified axial and ray parenchyma cells together with obliterated sieve-tube (Fig. 8E,F). At the site VA, rays in the inner nonconducting phloem were noticeably wider and more multiseriate (Figs 4E,F, 8), giving a higher volume (30–32 % vs. 26–28 % at the site T1; Table 3; Fig. 5E,F). In conducting phloem, the ray and sieve-tube fraction remained unchanged compared with 5-year-old bark (Table 3; Fig. 5A–D,G,H). The decreasing trend in total rays, especially uniseriate ones, continued: at the site T1, 8–9 out of 13–14 rays per mm were uniseriate, while at the site VA 7–8 out of 11–12 were uniseriate (Table 3; Fig. 4A–D). Ray width in conducting phloem averaged close to 3 cells in both sites (Table 3; Fig. 4E,F). From 10 years onward, procumbent cells dominated ray composition. The axial parenchyma remained diffuse without distinctive features in the volcanic habitat (Fig. 8E,F).

Ontogenetic changes in phloem ray of main stems (trunks)

In *B. ermanii*, young trunks or large branches (20–35 years) showed comparable stem diameters across habitats (Tables 2, 3; Fig. 2). The nonconducting phloem accounted for 70–80 % of total bark width (Table 3; Fig. 9C,D). All parenchyma in this zone were dilated, more strongly in the outer layers (Fig. 9C–F). In the inner nonconducting phloem, ray dilation occurred mainly by cell enlargement and less frequently by cell division, while in the outer layers cell division was dominant. In cross-section, rays in the inner nonconducting phloem became wavy (Fig. 9C–F). Broad wedge-shaped rays appeared in the central part of the nonconducting phloem, but unlike in younger bark, they did not determine the overall structure (Fig. 9C–F). Annual layering was visible in the inner nonconducting phloem, extending back 10–15 years, marked by alternating zones of

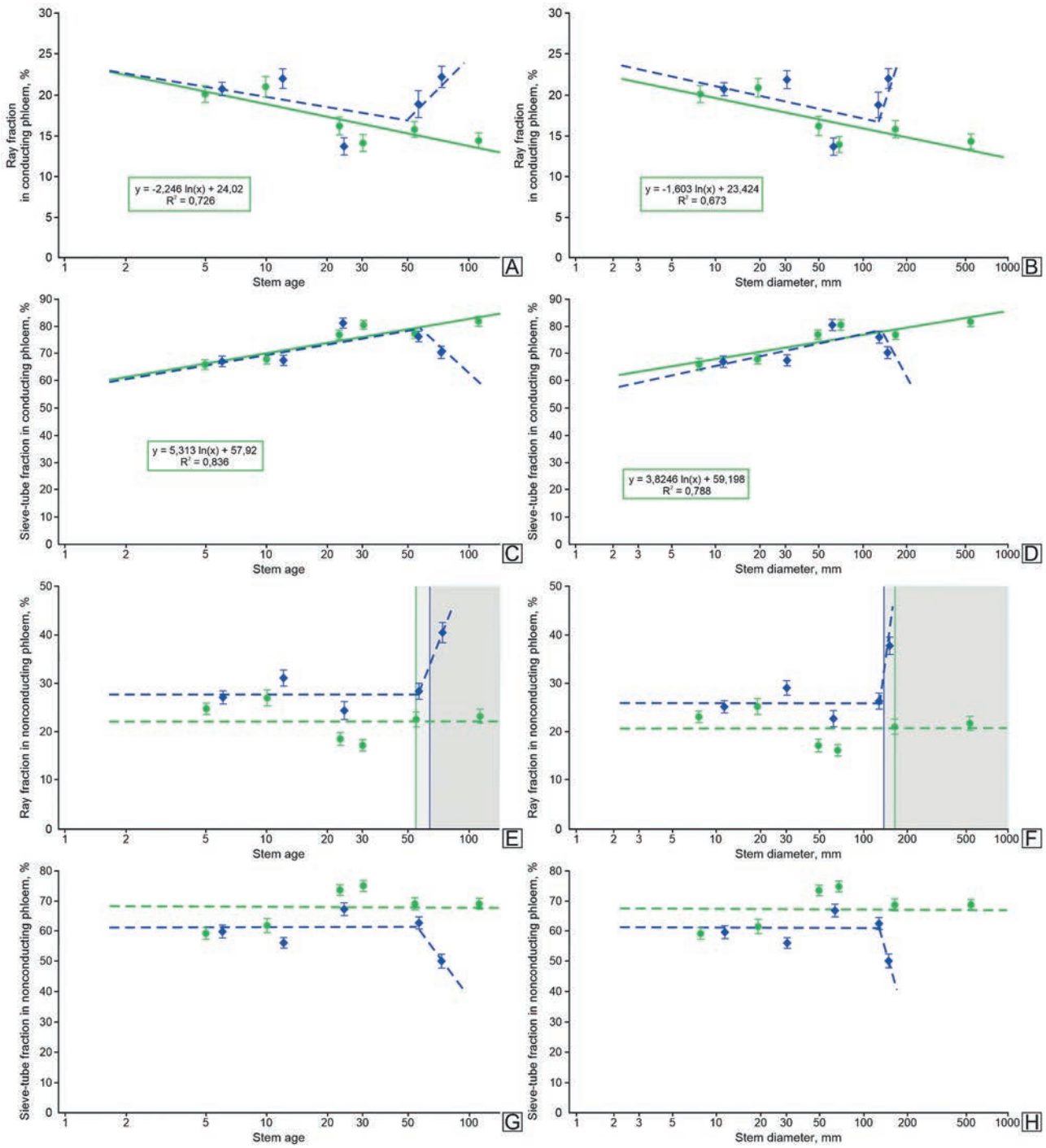

Figure 5 Relationships between phloem ray & sieve-tube fractions and tree age and stem diameter of *Betula ermanii* Cham. from southern Sakhalin and Iturup Islands: A, B – ray fraction in conducting phloem, %; C, D – sieve-tube fraction in conducting phloem, %; E, F – ray fraction in nonconducting phloem (inner bark), %; G, H –sieve-tube fraction in nonconducting phloem (inner bark), %; green lines are typical sites (T1 and T2) on Krasnaya Mt & Bolshevik Mt, Susunai Range, Sakhalin Island; blue lines are the site VA on Baransky Volcano, Grozny Range, Iturup Island; grey areas are rhytidome development; log-linear regression for solid lines & schematic timeline for dotted lines; error bars show confidence interval (CI); regression equations and coefficient of determination (R^2) are given in boxes. The proportion of variance explained by this relationship below 0.67 is indicated by dotted lines (green and blue)

large sieve-tube lumens in early phloem and narrow bands of dilated axial parenchyma in late phloem (Fig. 9E–H). Sclereids occurred singly or in clusters of varying size (Fig. 9C–F). Toward the stem periphery, sclereid clusters became larger, forming a zone of sclerified nonconducting phloem (Fig. 9C–H). At the site T1, the ray fraction in nonconducting phloem was 17–18 %, and the sieve-tube fraction 72–75 %, whereas at the site VA these values were 23–24 % and 65–69 %, respectively (Table 3; Fig. 5E–H). In conducting phloem, ray fractions were lower: 12–17 % at the site T1 and 13–14 % at the site VA (Table 3; Fig. 5A,B). In contrast, sieve-tube fractions in conducting phloem exceeded those in nonconducting phloem at both sites, reaching 75–81 % (Table 3; Fig. 5C,D,G,H). The total

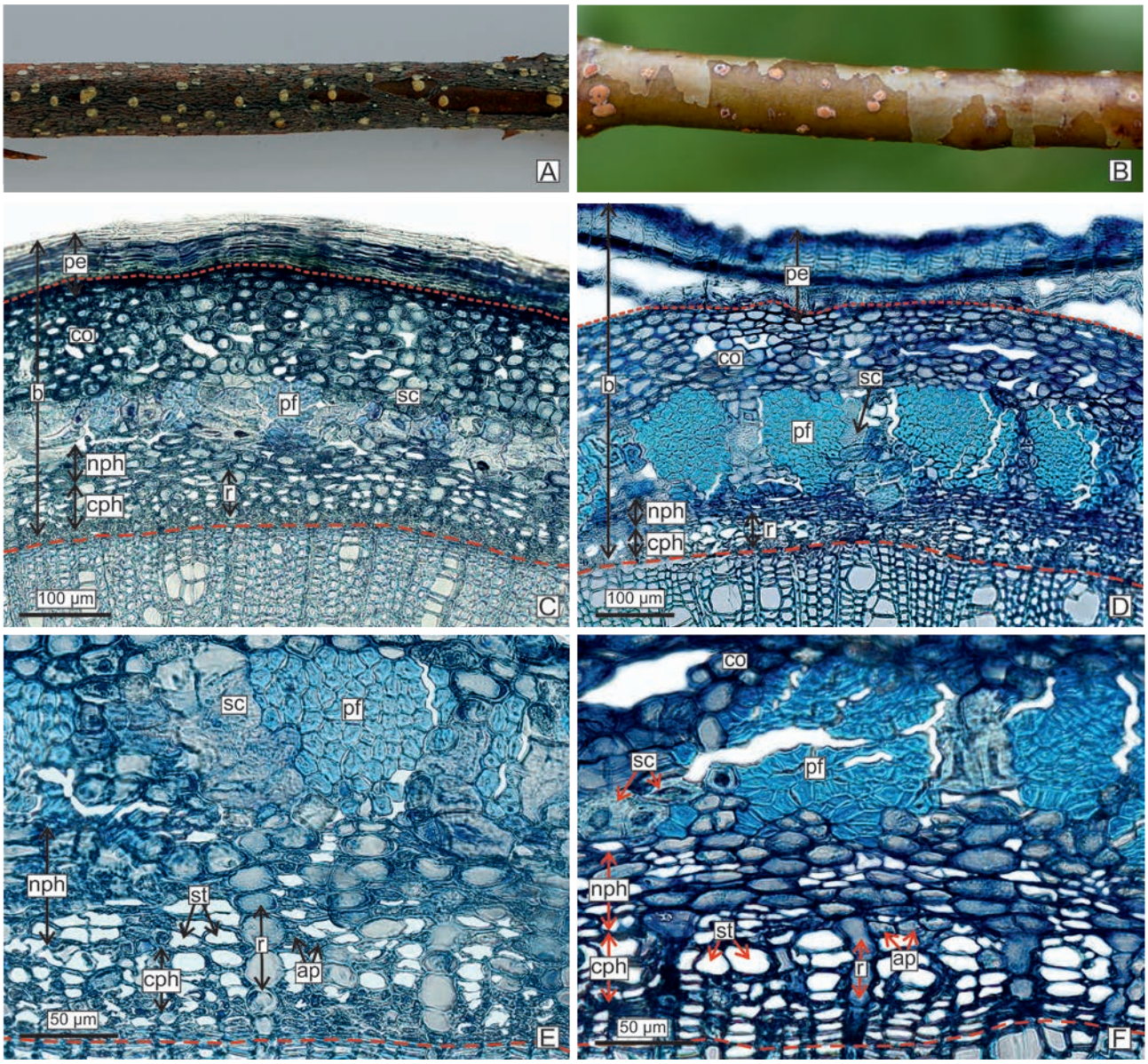

Figure 6 Bark of 2-yr old stems of *Betula ermanii* Cham. from southern Sakhalin and Iturup (site VA) Islands: A, C, E – site T1; B, D, F – (site VA); A, B – outer surface of stem bark; C, D – bark; E, F – inner bark zone; transverse section; red small dotted line is a phellogen; red dotted line is a vascular cambium. Abbreviations as in the Fig. 3

number of conducting phloem rays, including uniseriate rays, decreased: at the site T1 there were 10–11 rays per mm (5–6 uniseriate), while at the site VA there were 8–9 rays per mm (4–5 uniseriate) (Table 3; Fig. 4A–D). Average ray width in conducting phloem was 3–3.5 cells (Table 3; Figs 4E,F, 9G,H). Ray height was about 250 µm.

Trunks older than 54–56 years differed markedly in diameter between habitats, unlike branches (Tables 2, 3; Fig. 2). By 70 years, main stems at the site T1 were nearly twice as wide as those in the volcanic habitat. Logarithmic models of stem diameter versus age, and vice versa, indicated that these differences increased with time (Tables 2, 3; Fig. 2). In such trunks, rhytidome developed at the bark periphery (Figs 3, 6–9A,B, 10), first appearing at the site T1 in 54-year-old bark (Fig. 10C) and at the site VA in 63-year-old bark (Fig. 10E), despite stem diameter differences, as new periderms formed deep in the peripheral nonconducting phloem (Fig. 2). The nonconducting phloem accounted for 80–95 % of bark width (Table 3). Dilation and sclerification in mature bark were diffuse and uneven in axial parenchyma and rays (Figs 10D,E, 11A,B). In outer nonconducting phloem, axial parenchyma dilated mainly through cell division, with minimal cell enlargement, while in inner layers dilation was primarily by cell enlargement. Toward the periphery, cell division and enlargement occurred at similar rates. At the site VA, dilation of peripheral nonconducting phloem was more pronounced than at the sites T1 or T2 (Figs 10D,E, 11A,B). Unlike typical sites, wedge-shaped zones of dilated nonconducting phloem parenchyma were common at the site VA, visible in cross-section between large sclereid clusters (Figs 10E, 11B,D). These zones included one or more dilated rays and involved cortex or pseudocortex tissues. Here, axial parenchyma dilation exceeded ray dilation, while in the inner bark, ray dilation predominated (Fig. 11B,D).

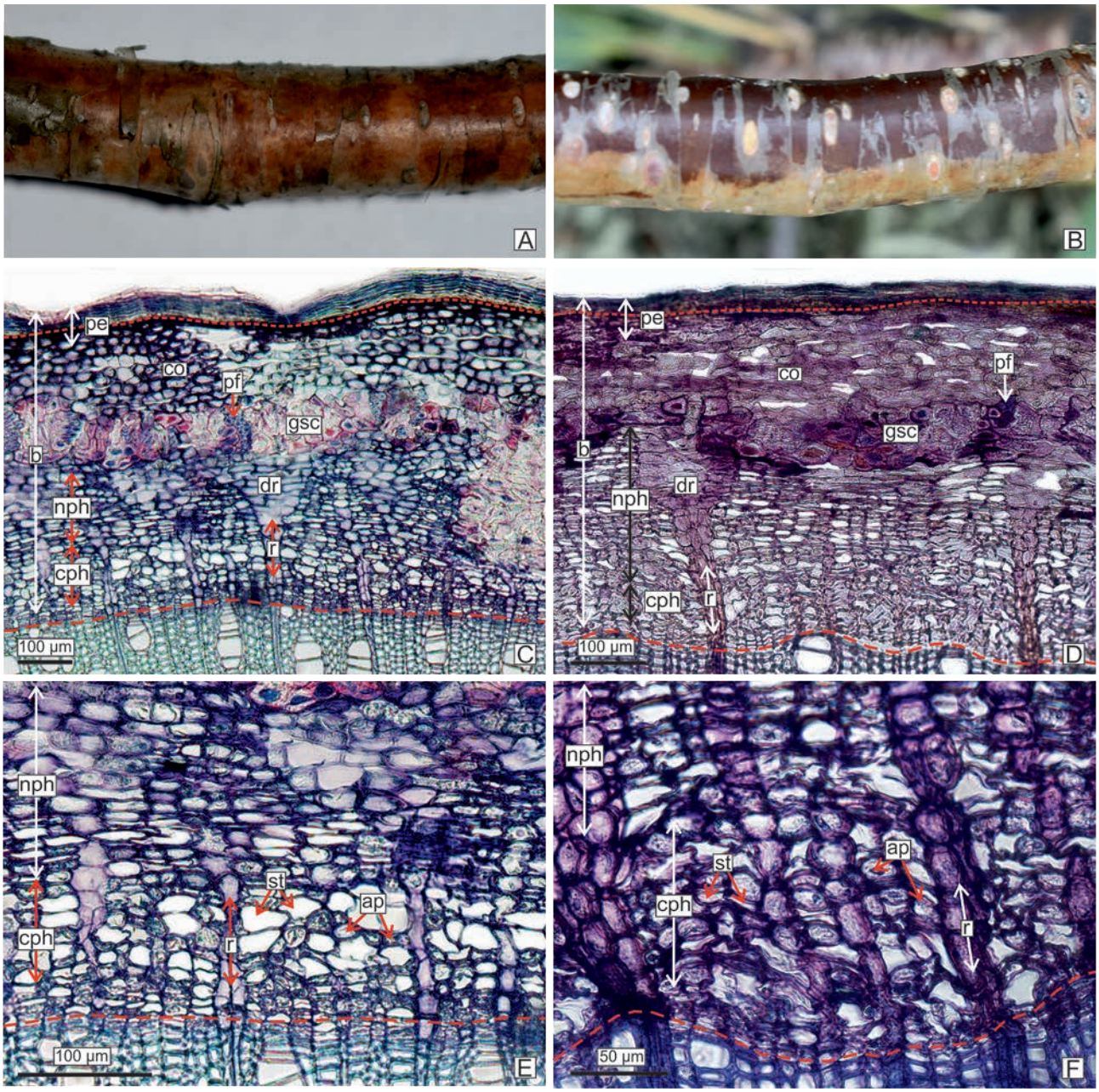

Figure 7 Bark of twigs of *Betula ermanii* Cham. from southern Sakhalin and Iturup (site VA) Islands: A, C, E – 5-yr old stem, site T1; B, D, F – 6-yr old stem, site VA; A, B – outer surface of stem bark; C, D – bark; E, F – inner bark zone; transverse section; red small dotted line is a phellogen; red dotted line is a vascular cambium. Abbreviations as in the Fig. 3

Axial parenchyma dilation was confined to sclerified zones where sclereid groups formed. At the site VA, ray width increased markedly in the transition from conducting to nonconducting phloem, driven by cell division, giving rays a bottle-shaped profile in cross-section (Fig. 11B,D).

At the site VA, the ray fraction increased 1.6-fold in conducting phloem and 1.7-fold in nonconducting phloem, reaching 21–23 % and 39–41 %, respectively (Table 3; Fig. 5A,B,E,F). Conversely, sieve-tube fractions declined (Table 3; Fig. 5C,D,G,H). Ray heights in conducting phloem of mature stems ranged from 170 to 200 µm. In nonconducting phloem, ray fractions increased steeply with age at the site VA but remained stable at typical sites (Table 3; Fig. 5E,F). Corresponding sieve-tube fractions followed opposite trends (Fig. 5G,H). In conducting phloem, divergence in ray and sieve-tube fractions between sites was evident only in mature bark (Table 3; Fig. 5A–D).

In conducting phloem of trunks older than 54–56 years, the total number of rays, including uniseriate rays, reached their lowest values across the lifespan and was similar between sites: 8–9 rays per mm, of which 4–5 were uniseriate (Table 3; Fig. 4A–D). In 73-year-old bark at the site VA, the number of uniseriate rays in conducting phloem dropped further to 2–3 per mm (Table 3; Figs 4C,D).

Age- and stem diameter-dependent regression of phloem ray traits

Regression analysis of ray traits against age and stem diameter revealed broadly similar trends across habitats (Fig. 2). The total number of rays and uniseriate rays in

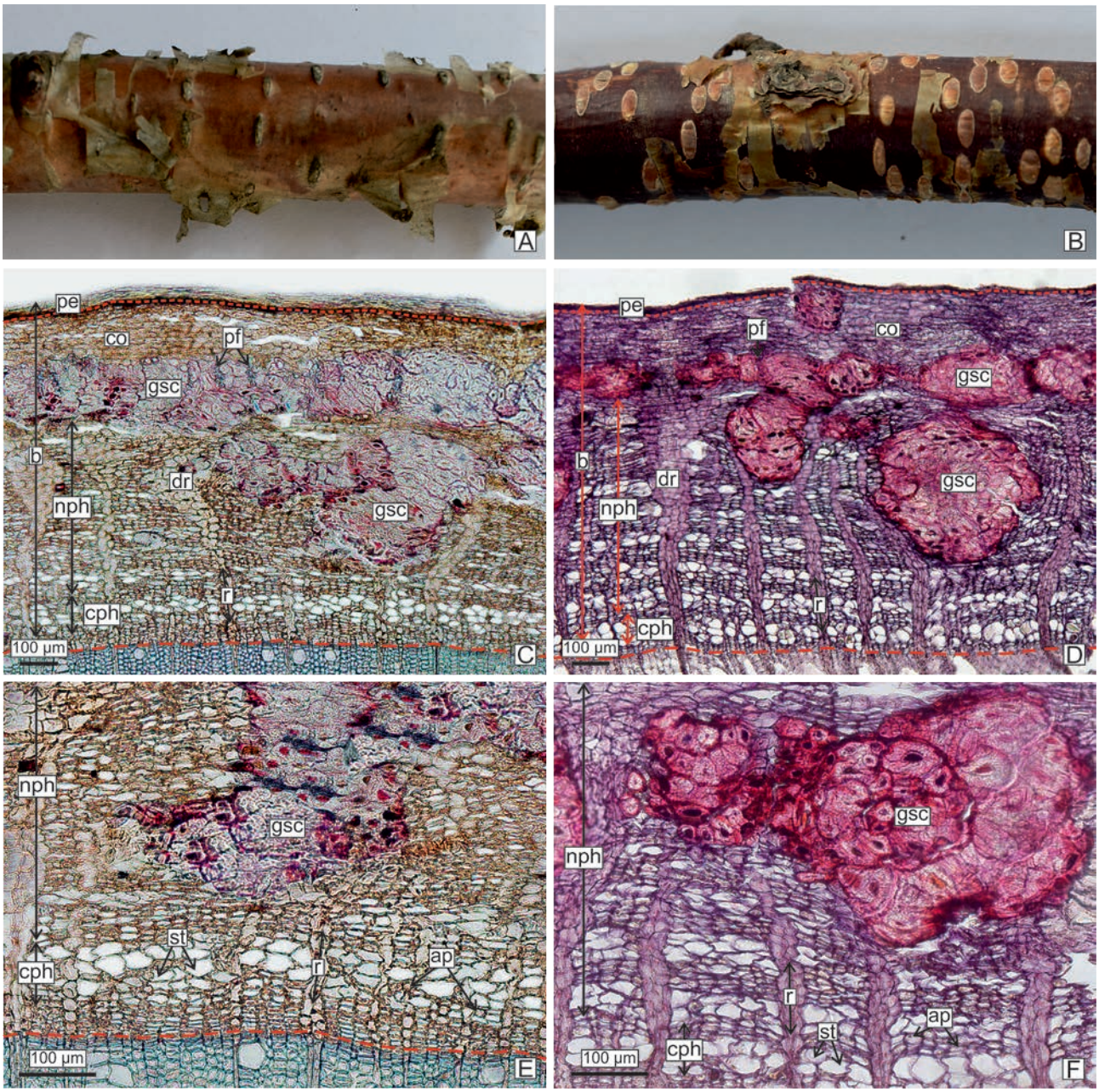

Figure 8 Bark of branches of *Betula ermanii* Cham. from southern Sakhalin and Iturup (site VA) Islands: A, C, E – 10-yr old stem, site T1; B, D, F – 12-yr old stem, site VA; A, B – outer surface of stem bark; C, D – bark; E, F – inner bark zone; transverse section; red small dotted line is a phellogen; red dotted line is a vascular cambium. Abbreviations as in the Fig. 3

the conducting phloem decreased logarithmically in both volcanic and typical sites, up to 24 years at the site VA (R^2 = 0.916 and 0.890) and in typical sites (R^2 = 0.917 and 0.947) (Fig. 4A,C). Comparable relationships with stem diameter were observed up to 69 mm at the site VA (R^2 = 0.858 and 0.824) and in typical sites (R^2 = 0.851 and 0.894) (Fig. 4B,D). Beyond these thresholds, ray numbers in the conducting phloem stabilised, both in young trunks at the site VA and in mature trunks at typical sites (Fig. 4A–D). Timelines for these traits at the site VA were consistently lower, although significant differences emerged only at certain ages (Fig. 4A–D).

In mature trunks, ray width in the conducting phloem reached no more than three cells at the site VA, compared to 3.5–4 cells in typical sites (Fig. 4E,F). Ray width followed a logarithmic relationship with age and stem diameter at both habitats (R^2 = 0.801 and 0.799 in typical sites; R^2 = 0.826 and 0.813 at the site VA), with similar overall values (Fig. 4E,F).

Fractions of rays and sieve-tube in the conducting phloem also followed a logarithmic model in the typical habitat (R^2 = 0.726 and 0.836 for age; R^2 = 0.673 and 0.788 for stem diameter) (Fig. 5A–D). At the site VA, the same tendencies were evident – a slight decrease in the ray fraction and an increase in sieve-tube – but with weaker explanatory power (R^2 < 0.67).

In the nonconducting phloem, ray and sieve-tube fractions remained constant with increasing age and stem diameter in the typical habitat, whereas at the site VA they rose sharply in large-diameter, older trunks, beginning even before sequent periderms formed the rhytidome (Fig. 5E–H).

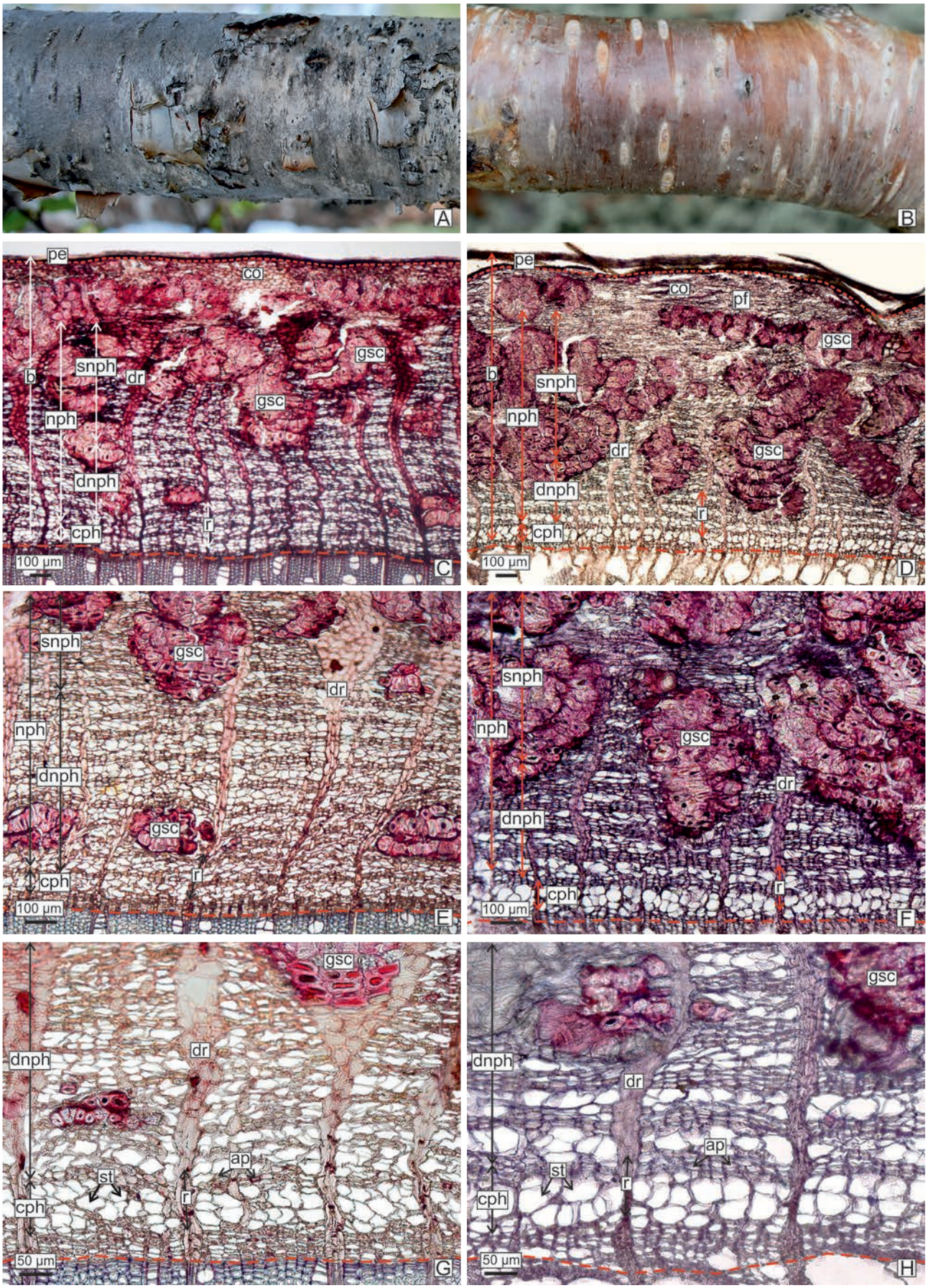

Figure 9 Bark of branches and young main stems (trunks) of *Betula ermanii* Cham. from southern Sakhalin and Iturup (site VA) Islands: A, C, E, G – 23-yr old stem, site T1; B, D, F, H – 24-yr old stem, site VA; A, B – outer surface of stem bark; C, D – total bark; E, F – middle and inner bark zone; G, H – inner bark zone; transverse section; red small dotted line is a phellogen; red dotted line is a vascular cambium. Abbreviations as in the Fig. 3

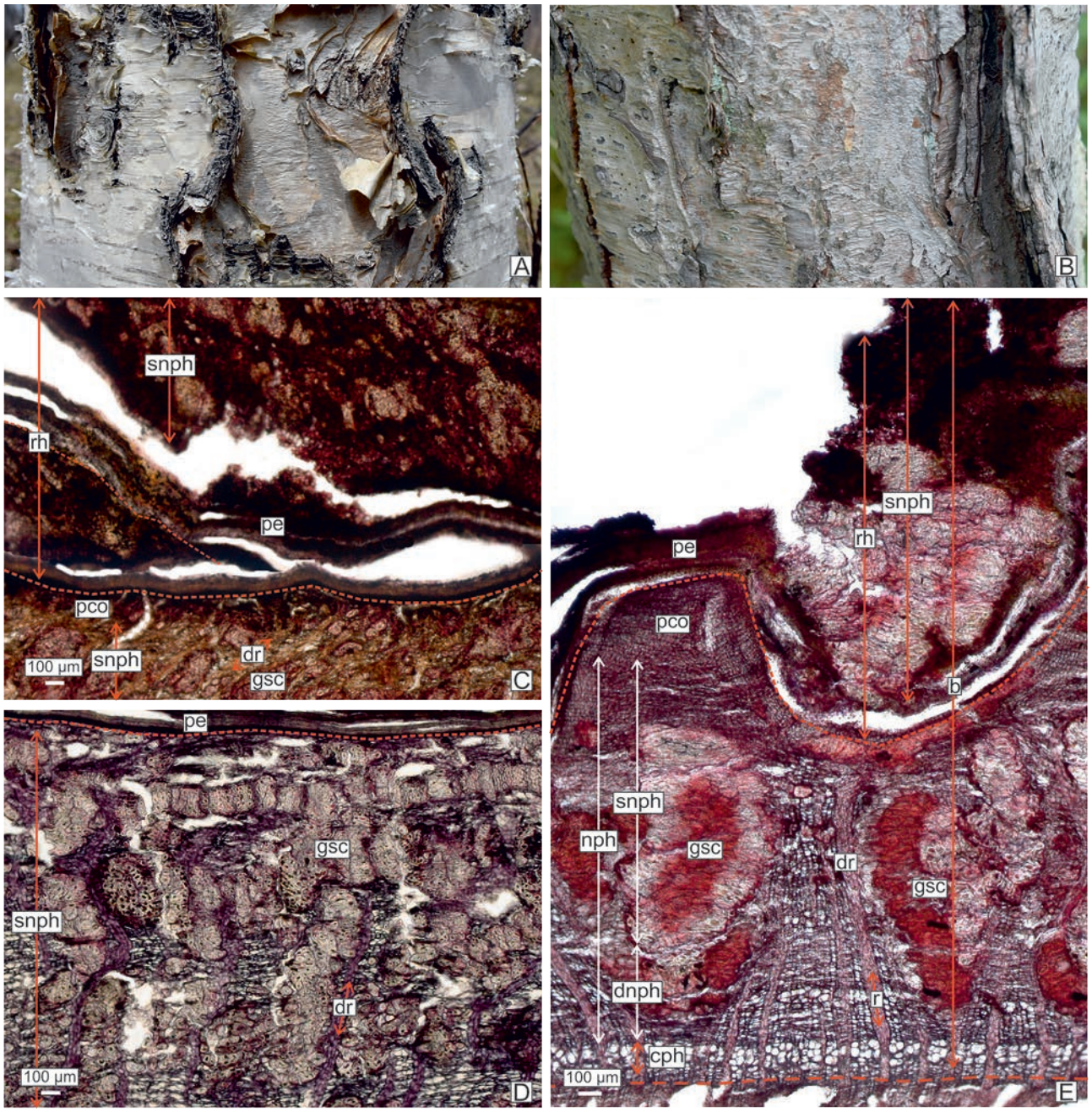

Figure 10 Outer mature bark of *Betula ermanii* Cham. main stems (trunks) from southern Sakhalin and Iturup (site VA) Islands: A, C, D – site T1; B, D, F – site VA; A – 63-yr old bark, outer surface of bark; B – 80-yr old bark, outer surface of bark; C – 69-yr old bark, outer bark zone; D – 54-yr old bark, outer & middle inner bark zone; E – 73-yr old bark, total bark; transverse section; red small dotted line is a phellogen; red dotted line is a vascular cambium. Abbreviations as in the Fig. 3

DISCUSSION

Stem diameter vs. tree age patterns: drivers of phloem parenchyma changes

A linear increase in bark width and nonconducting phloem with age has been reported for *B. ermanii* across different habitats (Kopanina et al. 2022). One might expect stem diameter to increase in a similar manner. However, our results show that stem diameter in *B. ermanii* increases with age and height according to a logarithmic model, with a high coefficient of determination (Fig. 2). Age and stem diameter (twigs, branches and trunks) were logarithmically related (R^2 = 0.985 at the typical site; R^2 = 0.958 at the site VA) (Fig. 2). It should be noted that the relationship between age and stem diameter at older ages under typical conditions was almost linear (Fig. 2). We suggest that this may be related to more favourable light conditions for trees at site T2. These trends indicate that diameter growth is much faster at young ages than in mature trees (Fig. 2). A similar non-linear pattern was noted in forestry studies, where birch was described as fast-growing in height during the first 15–20 years, while diameter growth lagged (Manko 1967, Kabanov 1972).

In the volcanic habitat, stem diameter trends had two distinct features: higher growth rates in twigs and branches (young stems), but lower rates in mature trunks (Fig. 2). We

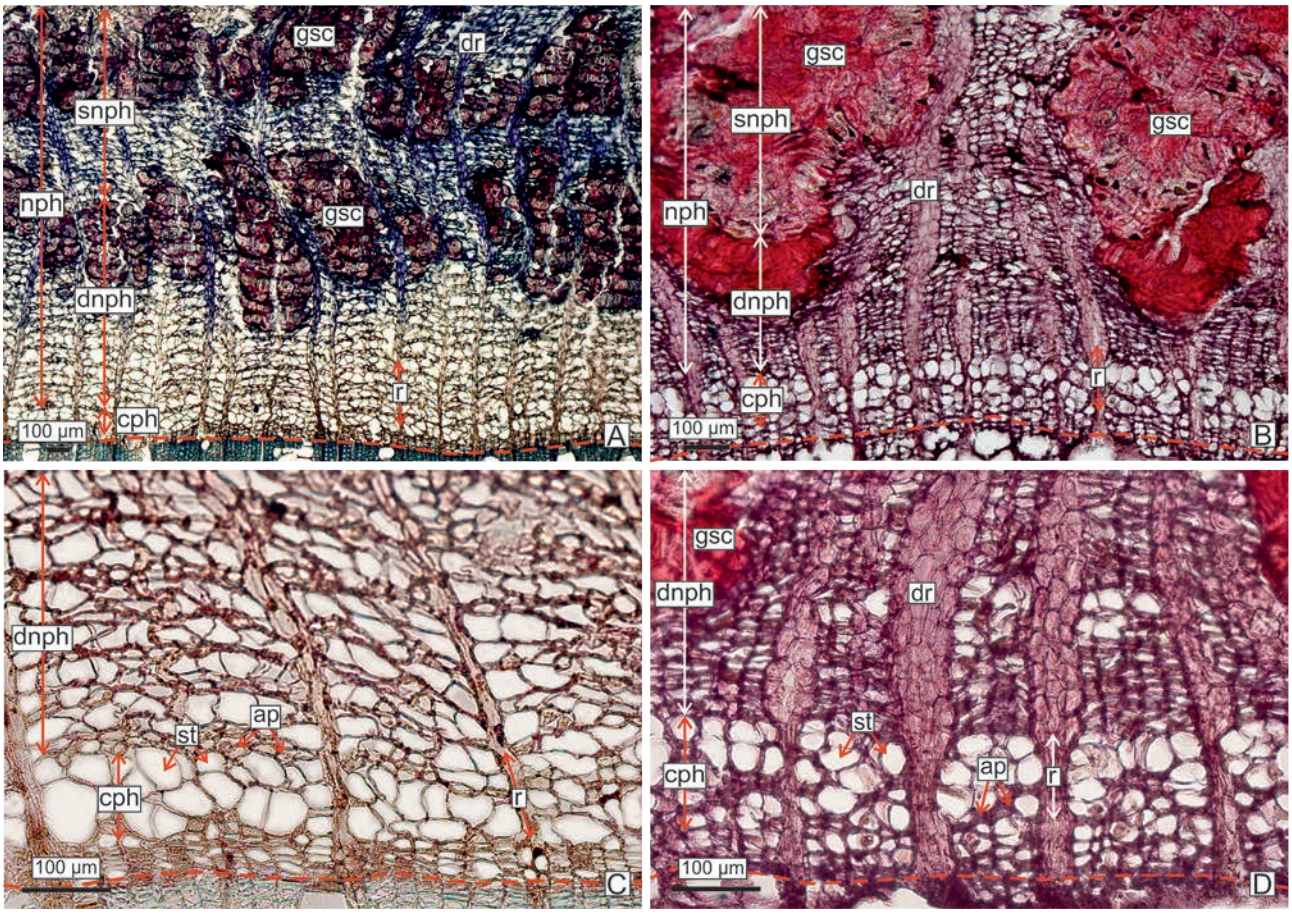

Figure 11 Inner mature bark of *Betula ermanii* Cham. main stems (trunks) from southern Sakhalin and Iturup Islands: A, C – 54-yr old bark from the site T1; B, D – 73-yr old bark rom the site VA; A, B – middle & inner bark zone; C, D – inner bark zone; transverse section; red dotted line is a vascular cambium. Abbreviations as in the Fig. 3

suggest that large diameters of young stems in this environment reflect compensatory growth following crown damage.

The relationships between stem diameter and age under contrasting conditions highlight differences not only in growth rates but also in ray trait patterns between crown twigs and branches vs. main stems (mature trunks) (Figs 4, 5). Given the consistently high regression coefficients for both age and diameter (Figs 2, 4, 5), our data do not allow us to identify one factor as the dominant driver. Because studies explicitly addressing whether age, diameter, or height best explains phloem parenchyma or sieve-tube variation remain scarce (Quilhó et al. 2000, Savage et al. 2017, Losada & Holbrook 2019, Clerx et al. 2020), and because phloem function is tightly coupled with xylem (Pfautsch et al. 2015), we drew on more extensive xylem studies for interpretation.

In wood anatomy and functional ecology, the problem of separating age and diameter effects is well recognised, as both influence tissue structure, especially ray and axial parenchyma (von Arx et al. 2015). Tree age and trunk diameter/height are strongly correlated: older trees tend to be larger, but the relative rates of diameter and height increment vary by species, individuals, and conditions (von Arx et al. 2015, Meng et al. 2021). This complicates interpretation, since disentangling mechanical effects of increasing diameter from age-related changes in cell programmes is difficult without targeted experiments.

Evidence from xylem indicates that diameter exerts the more direct effect. It influences tracheid conductivity (Spicer & Gartner 2001) and the distribution, density, and size of rays (Meng et al. 2021, Rungwattana & Hietz 2018). With increasing diameter, ray fraction and dimensions typically rise, while ray density falls – a pattern explained as a functional adjustment to greater mechanical load, longer transport pathways, and increased storage demand (Meng et al. 2021, Rungwattana & Hietz 2018). Thus, stem diameter is often interpreted as the stronger predictor of xylem ray variation compared with age. This interpretation is supported by direct statistical tests comparing age and diameter as drivers of radial variation (Rungwattana & Hietz 2018). At the same time, those authors emphasised that strong correlations between diameter and age (R^2 = 0.64–0.77) make it difficult to fully separate their effects. A comparable conclusion was reached in analyses of phloem and xylem hydraulic traits in relation to stem height and diameter (Jyske & Hölttä 2015). Under very strong collinearity (R^2 = 0.93), local diameter provided only partial explanatory power for variation in conductive element dimensions in both tissues.

In our data for *B. ermanii*, the correlation between age and stem diameter exceeded 0.96, with unique size variation accounting for less than 4 % (Fig. 2). Under such conditions, the statistical power to detect a "pure" effect of diameter at fixed age is extremely low. However, the absence of statistical significance for the size predictor should not

be taken as evidence of no biological effect. In practice, our data do not allow a meaningful separation of age and diameter effects.

Age, by contrast, is more commonly used as a key factor in characterising ontogenetic stages of transport tissues. Differences in xylem and phloem across ages are linked to cambial structural changes (Pfautsch et al. 2015, Onyenedum & Pace 2021, Lev-Yadun 2025). We discuss our results in relation to cambial age later in the text. Some studies identify age as the primary driver of xylem hydraulic traits (Li et al. 2019), while others emphasise age together with height as closely linked predictors (Park et al. 2009). In such cases, part of the observed variation may reflect differences in stem diameter and plant height.

Accordingly, in studies of xylem and phloem structure, the choice between age and stem diameter depends on the framework adopted: hydraulic hypotheses often use local diameter and axial position as mechanistic predictors, whereas the ontogeny of transport tissues as cambial derivatives is more appropriately described in terms of age.

Ontogenetic transitions of phloem rays: from crown twigs and branches to main stems

Bark tissue transformations in *B. ermanii* from the age of 5 years onward – including dilatation, sclerification, and the formation of sequent periderms – occurred at similar ages across the study sites despite differences in stem diameter (Figs 7–10). Variation in phloem traits during ontogeny is closely linked to increasing parameters of tree habitus: age, height, and stem diameter. A direct positive allometric correlation is well documented between plant height (length of the transport pathway) and both the width and length of sieve-tube elements, for phloem (Jyske & Hölttä 2015, Savage et al. 2017, Losada & Holbrook 2019, Kopanina & Vlasova 2019, Clerx et al. 2020, Kopanina et al. 2022, Tarelkina et al. 2024) and for tracheids or vessel members in xylem, regardless of climate or life form (Olson et al. 2020, 2021, Onyenedum & Pace 2021).

The vascular cambium, producing secondary xylem (wood) and secondary phloem (inner bark), underlies secondary growth and axial organ thickening (Evert 2006, Pfautsch et al. 2015, Onyenedum & Pace 2021, Lev-Yadun 2025). Because phloem and xylem share developmental origins and functional roles in solution transport, data on wood rays are relevant for interpreting phloem rays. Our study shows that the allometric correlations identified for xylem rays (Onyenedum & Pace 2021) also apply to phloem ray traits in *B. ermanii*.

Across ontogeny, bark supports carbon transport via the phloem, photosynthesis in parenchyma, and protection from the environment (Wittmann & Pfanz 2007, Pfautsch et al. 2015, Vandegehuchte et al. 2015, Alonso-Serra et al. 2019). Carbon transport involves long-distance flow through sieve-tube and radial redistribution via parenchyma (Esau 1953, 1977, Evert 2006, Pfautsch et al. 2015, Van Bel 2021). Phloem rays, together with axial parenchyma, cortex, and phelloderm, form the short-distance transport pathway toward sinks in actively dividing tissues (Evert 2006, Pfautsch et al. 2015, Van Bel 2021). The age-related changes in phloem rays observed in both volcanic and reference sites therefore indicate functional shifts in carbon allocation between young and mature bark.

Xylem ray width, composition, and conductive elements vary with age, reflecting the activity of ray and fusiform initials (Evert 2006, Pace & Angyalossy 2013, Pace et al. 2015, Onyenedum & Pace 2021). Similarly, in *B. ermanii* sieve-tube elements enlarged and clustered with age (Kopanina et al. 2022), increasing conducting phloem width (Table 3, Figs 3, 6–9, 10A,B). Ray traits of conducting phloem showed parallel ontogenetic shifts.

Consistent with Carlquist's (2001) hypothesis, young, narrow stems produce upright and square ray cells favoring axial transport, whereas older, wider stems produce predominantly procumbent cells supporting lateral flow. In *B. ermanii*, procumbent cells became predominant from 10 years of age in both volcanic and reference habitats. During the same period, uniseriate rays decreased by half, while 2–3-seriate rays became common (Table 3, Fig. 4C–F). Ray width increased logarithmically with age, as in many trees (Evert 2006), but in *B. ermanii* it did not exceed 3–3.5 cells even in 100-year-old trunks, comparable to values in 10–20-year-old stems (Table 3, Fig. 4E,F).

With age, in *B. ermanii*, the total number of rays in conducting phloem decreased in both environments (Table 3, Fig. 4A,B). Structural traits of sieve-tubes and rays followed logarithmic patterns early in ontogeny, with sieve-tube traits increasing (Kopanina et al. 2022) and ray traits decreasing (Figs 4, 5A–D). Only ray width increased logarithmically (Fig. 4E,F). Ray/sieve-tube fractions also showed opposite logarithmic trends (Fig. 5A–D). These patterns highlight faster changes in crown twigs and branches than in main stems (Figs 4, 5), consistent with the species' rapid early growth.

Importantly, strong logarithmic trends in ray traits were evident only in young bark of *B. ermanii* up to 25–35 years old (Figs 4, 5A–D). In mature and old bark, the traits reached a plateau. This indicates that the early developmental trajectories of phloem rays in twigs and branches cannot be directly extrapolated to main stems. Similar ontogenetic patterns have been documented in rays (Khan et al. 1981, Tsuchiya & Furukawa 2010) and in axial wood systems of many woody species (Khan et al. 1981, Carlquist 2001, von Arx et al. 2015, Pace et al. 2018, Onyenedum & Pace 2021).

Phloem ray traits: functional implications and adaptive signals under volcanic stress

The age-related trends in the total number of phloem rays, including uniseriate rays, in the conducting phloem of *B. ermanii* showed that values at the site VA (Baransky Volcano) were significantly lower – by 1.4 to 2 times – than at typical sites (Table 3, Fig. 4A–D). Moreover, the extent of decrease from 1-year-old to mature bark differed: at the typical site, the total number of rays declined threefold, while at the site VA it decreased 2.8 times. For uniseriate rays, the decline was even more pronounced – 6.2-fold at the typical site and 9.3-fold at the volcanic site (Table 3, Fig. 4A–D). The response to volcanic stress became evident as early as 5 years, when the ratio of nonconducting to conducting phloem width increased 5.5 times at the volcanic

site compared with 3 times at the typical site (Figs 4, 5). At this stage, the proportion of uniseriate rays fell to 55 % at the site VA, while at the typical site it remained at 90 % of all rays (Table 3, Fig. 4A–D). Only in mature bark at the typical site did the proportion of uniseriate rays eventually drop to 52 %, whereas in the volcanic habitat it declined further to 30 % by 73 years (Table 3, Fig. 4A–D). From 25–35 years onward, the number of rays in the conducting phloem reached a plateau in both environments (Table 3, Fig. 4A–D). This occurred despite the fact that mature main stems (trunks) in volcanic habitats were 1.7 times smaller in diameter than those from the typical site. Similar decreases in ray numbers, interpreted as a nonspecific stress response, have also been reported in the secondary xylem of Arctic shrubs and dwarf shrubs (Chavchavadze & Sizonenko 2002). In *Pinus sylvestris* L., reductions in axial phloem parenchyma were recorded under industrial and recreational stress in the suburbs of Krasnoyarsk (Skripalshchikova et al. 2009). By contrast, increases in the number of xylem and phloem rays under chronic aeropollution from large industrial facilities in Krasnoyarsk were clearly induced by heavy metal emissions (Sr, Zn, Ni, Cr) in *Betula pendula* Roth (Stasova et al. 2011, 2013).

The increase in ray width with age in the conducting phloem did not differ significantly between sites, although notable differences were recorded in specific years (1, 5, and 54–73 years) (Table 3, Fig. 4E,F). The number of rare large (4-seriate) rays in the conducting phloem also did not differ significantly between sites. However, their abundance was consistently lower at the site VA than at the typical site.

Age-related trends in the fractions of rays and sieve-tubes in the inner bark – within both the conducting and nonconducting phloem – were particularly striking in the volcanic habitat (Fig. 5). In mature trunks at the site VA, ray fraction increased 1.3–1.5 times, while the fraction of sieve-tubes in the conducting phloem decreased accordingly. In contrast, under typical conditions the ray fraction in the conducting phloem decreased by 70 % from 1-year-old to old bark (Table 3, Fig. 5A,B). Conversely, in the volcanic environment, ray fraction in mature stem bark increased by 94% relative to 1-year-old bark (Fig. 5A,B). In young bark, ray and sieve-tube fractions were nearly identical across habitats (Fig. 5A–D).

A markedly different pattern was observed in the nonconducting phloem. At the site VA, ray fraction was 1.5 times greater than at typical sites, while sieve-tube fraction decreased (Fig. 5E–H). During growth in the volcanic habitat, ray fraction in old bark increased by 1.5 times compared with 1-year-old bark, whereas at typical sites such changes were negligible (Fig. 5E,F). This trend is vividly reflected in transverse sections, where phloem rays often acquired a bottle-shaped form due to active dilation, visible in young trunks around 20 years old and in older ones (Figs 9C–H, 10E, 11). At the same time, mature trunks at the volcanic site had significantly smaller diameters than those at the typical site.

We therefore argue that our results reveal deviations from normal ontogenetic changes of phloem parenchyma in the inner bark (conducting and nonconducting phloem) under volcanic stress. We propose that the increase of phloem parenchyma, at the expense of nonconducting phloem, represents an adaptive response. Structural changes in phloem rays may result from coordinated adjustments in short-distance transport within bark tissues and wood of *B. ermanii*, improving resistance to drought-induced vessel embolism. The development of dilated parenchyma areas may thus be triggered not only by girth growth but also by environmental stressors such as drought or physiological drought caused by salinity.

In this context, Lintunen et al. (2016) demonstrated in living bark samples of adult *Pinus sylvestris*, *Picea abies* (L.) H. Karst., *Betula pendula*, and *Populus tremula* L. across Europe – from boreal Finland to Mediterranean Portugal – that variation in secondary phloem water content is age-dependent. Phloem osmolality increased under drought or cold stress, with both conifers and angiosperms regulating water content while solute levels remained stable (Lintunen et al. 2016). Fire effects provide further evidence: in *Pinus sylvestris* forests of the Lower Priangarie, low-intensity fires caused an increase in phloem ray frequency, unlike medium- and high-intensity fires (Stasova et al. 2020).

Studies of drought-induced embolism in xylem vessels emphasize the importance of parenchyma: a high proportion of axial parenchyma and xylem rays supports vessel integrity and hydraulic stability (Nardini et al. 2011, Plavcova et al. 2016, Morris et al. 2018). In drought-prone limestone areas of China, xylem hydraulic traits in 19 temperate broadleaf species were closely linked to axial parenchyma, particularly paratracheal parenchyma (Chen et al. 2020). On a subtropical island in Japan, xylem parenchyma of 15 woody species showed strong associations with hydraulic function and carbohydrate storage, with both ray and axial parenchyma playing a key role under conditions of low cavitation resistance (Kawai et al. 2021). Recent studies in subtropical montane angiosperms demonstrated that drought adaptation involves not only immediate resistance to embolism but also recovery of embolised vessels (Zhang et al. 2024). A large-scale analysis of 173 tropical tree species along an elevational gradient on Mount Cameroon revealed that montane species are characterised by smaller vessels and abundant radial parenchyma, traits enhancing drought resistance. Notably, their scarcity of axial parenchyma is compensated by rays composed of upright and square cells (Plavcová et al. 2024). These features parallel those of *B. ermanii*, adapted to a cool temperate maritime climate. We suggest that the increased ray fraction observed in *B. ermanii* under volcanic stress represents a functional adaptation comparable to those found in woody plants across diverse drought- and salt-affected regions.

Finally, a global analysis of over 2000 woody angiosperms showed a consistent association between xylem conducting elements and axial parenchyma, but not with ray parenchyma (Morris et al. 2018). This suggests contrasting functional strategies: axial parenchyma co-adapts with conductive elements for vertical long-distance transport, whereas ray parenchyma is specialised for radial transport. Moreover, fine-tuned interactions between xylem and phloem – mediated primarily by ray parenchyma – are crucial for short-distance water transfer from phloem to drying xylem

(Nardini et al. 2011, Pfautsch et al. 2015, Sevanto 2018).

The bark parenchyma, particularly the phloem parenchyma, is multifunctional, with resource storage as one of its key roles (Evert 2006). Isotopic studies confirm that nonstructural carbohydrates in phloem parenchyma are central to maintaining transport balance across forest ecosystems (Richardson et al. 2013, Plavcova & Jansen 2015, Hartmann & Trumbore 2016, Plavcova et al. 2016, Furze et al. 2018, Inagawa et al. 2023). In tree stems, substantial sugar storage and exchange with older reserves indicate that stems regulate not only long-distance transport but also overall carbon balance (Richardson et al. 2013, Hartmann & Trumbore 2016, Furze et al. 2018). In tropical forests, savannas, and rainforests, the inner bark contributes 17–36 % of nonstructural carbohydrate reserves (Rosell et al. 2020). At the whole-plant level, storage in bark parenchyma buffers asynchrony between demand and supply on diel to decadal scales (De Schepper et al. 2013, Hartmann & Trumbore 2016). In this framework, the enlarged rays in the nonconducting phloem near the cambium likely act as reservoirs of nutrients and water in *B. ermanii* stems under volcanic stress (Figs 4, 5, 9, 10E, 11), supporting sink tissues such as the vascular cambium and sapwood. Under stress, including drought, large trees can meet up to 22 % of daily water needs from parenchymal storage to offset transpiration losses (Steppe et al. 2015).

Another essential role of phloem parenchyma, particularly at the bark periphery, is photosynthesis, which supplies local carbon to sink tissues (Wittmann & Pfanz 2007, Vandegehuchte et al. 2015, Alonso-Serra et al. 2019). Thus, carbon starvation is not solely a matter of reserve size but also of local carbon availability for meristems and division zones (Vandegehuchte et al. 2015). CO_2 recirculation from bark photosynthesis can compensate 7–98 % of carbon losses in woody tissues, with a median of 72 % (Vandegehuchte et al. 2015). In volcanic habitats, we observed extensive zones of dilated peripheral parenchyma (nonconducting phloem, cortex, and phelloderm) in *B. ermanii* (Figs 9C–F, 10C–E). These tissues, critical for rhytidome initiation, developed later and at smaller stem diameters at the site VA compared to typical sites (Table 2, Figs 2, 10). Even stronger habitat differences were observed in nonconducting phloem width, which was more than twice as narrow under volcanic stress, despite representing the major living bark fraction (Table 3). This suggests that radial transport pathways are shorter in stressed trees, conserving resources. Combined with photosynthetic activity of peripheral bark parenchyma in large stems and branches, this likely provides additional carbon and water for *B. ermanii* in response to crown reduction (Table 1).

Ultimately, bark structure and function determine the adaptive potential and ecological strategy of trees. Functional traits of bark and transport systems in woody plants are thus key to identifying ecosystems and understanding their dynamics (Bruelheide et al. 2018).

CONCLUSION

Analysis of stem diameter variation with age showed that their relationship in *B. ermanii* is non-linear both in favorable environments, where it grows as a tall tree, and in stressful volcanic environments, where it remains low-growing. The increase in stem diameter during ontogeny followed a logarithmic law with high coefficients of determination. Our results suggest that, under volcanic stress, growth retardation occurs in mature trunks, in contrast to typical sites. These findings confirm earlier reports for many woody plants that habitus and both radial and axial systems derived from the vascular cambium are linked by direct positive allometric correlations.

Using statistical methods, we examined the structural responses of *B. ermanii* phloem rays to volcanic stress, which induces a state of physiological drought in trees growing near the thermal springs of Baransky Volcano on Iturup Island. By examining age-related trends, we were able to assess the rate and pattern of bark trait variation in contrasting environments. This approach, first introduced and applied to the study of volcanic stress by Kopanina et al. (2022), also helped us to circumvent the methodological difficulty of comparing plants of different ages and, consequently, different physiological states of the bark. The diversity and multifunctionality of bark, determined by ontogenetic and biomorphological features, present major challenges for ecological studies. We argue that analysing trait dynamics through age-related trends provides a robust framework for identifying structural patterns of bark variation across habitats and populations of different age structures.

Irrespective of environment, ontogeny of the conducting phloem in *B. ermanii* is characterised by a threefold decline in the total number of rays, including a six- to ninefold reduction in uniseriate rays; a shift in ray composition towards the predominance of procumbent cells from 10 years onward; and an increase in ray width to 3-seriate. These ontogenetic trends followed logarithmic patterns with high coefficients of determination up to 25–35 years in young bark and reached a plateau in mature bark. Such trends confirm earlier findings on age-related changes in ray traits in secondary xylem.

At the same time, our data reveal deviations from these reference ontogenetic trajectories in the volcanic environment. In young bark, the total number of rays, including uniseriate rays, was up to twofold lower compared to typical sites, whereas in mature bark values converged. We cannot yet explain this peculiarity, but suggest that it merits targeted study under other stress conditions. Another significant trend was the higher fraction of ray parenchyma (1.5–2 times) in the inner bark of mature trunks in volcanic habitats compared to typical sites. We propose that these additional ray fractions represent coordinated structural–functional changes enhancing radial transport and providing local sources of water and carbon in the inner bark of *B. ermanii*, thereby compensating for reduced crowns and physiological drought.

Our study demonstrates that phloem ray development in *B. ermanii* follows distinct patterns of ontogenetic change under volcanic stress. The accelerated decline of uniseriate rays, combined with a persistent increase in ray parenchyma fractions in the nonconducting phloem, highlights structural deviations from typical ontogenetic patterns. These deviations

likely reflect adaptive adjustments of radial transport and storage functions under conditions of physiological drought.

However, several unresolved questions remain. It is still unclear to what extent these changes in phloem parenchyma are coordinated with xylem traits, and how they contribute to whole-plant carbon and water balance. Addressing these questions will require integrative studies combining detailed anatomical data with physiological and ecological approaches. We therefore consider our results as a first step toward understanding the functional role of phloem rays in the adaptation of woody plants to complex volcanic stress regimes, and as a basis for future research into their broader ecological and evolutionary significance.

ACKNOWLEDGEMENTS

This work was carried out on government assignment of the Institute of Marine Geology and Geophysics FEB RAS. For consultations on statistical data processing methods, the authors express their gratitude to Ph.D. in physics and mathematics Valery V. Ershov. The authors also sincerely thank the reviewer for constructive comments and insightful suggestions, which have significantly improved the clarity and overall quality of the manuscript.

LITERATURE CITED

Alonso-Serra, J., O. Safronov, K.J. Lim, S.J. Fraser-Miller, O.B. Blokhina, A. Campilho, S.L. Chong, K. Fagerstedt, R. Haavikko, Y. Helariutta, … & J. Salojarvi 2019. Tissue-specific study across the stem reveals the chemistry and transcriptome dynamics of birch bark. *New Phytologist* 222:1816–1831.

Angyalossy, V., M.R. Pace, R.F. Evert, C.R. Marcati, A.A. Oskolski, T. Terrazas, E. Kotina, F. Lens, S.C. Mazzoni-Viveiros, G. Angeles, … & P. Baas 2016. IAWA list of microscopic bark features. *IAWA Journal* 37(4):517–615.

Ashburner, K. & H.A. McAllister 2016. *The genus Betula: a taxonomic revision of birches*. Reprinted with corrections. Royal Botanic Gardens, Kew, London, 432 pp.

Barkalov, V.Yu. 2009. *Flora of the Kuril Islands*. Dalnauka, Vladivostok, 466 pp. (in Russian). [Баркалов В.Ю. 2009. Флора Курильских островов. Владивосток: Дальнаука. 466 с.].

Barykina, R.P., T.D. Veselova, A.G. Devyatov, H.H. Dzhalilova, G.M. Ilina & N.V. Chubatova 2004. *Handbook of botanical micro-technology. Foundations and methods*. Izdatel'stvo MGU, Moscow, 312 pp. (in Russian). [Барыкина Р.П., Веселова Т.Д., Девятов А.Г., Джалилова Х.Х., Ильина Г.М., Чубатова Н.В. 2004. Справочник по ботанической микротехнике. Основы и методы. Москва: Изд-во МГУ. 312 с.].

Bragin, I.V., G.A. Chelnokov & N.A. Kharitonova 2019. Geochemistry of thermal springs at Baransky volcano, Southern Kuriles (Russia). *Environmental Earth Sciences* 78:79.

Bruelheide, H., J. Dengler, O. Purschke, J. Lenoir, B. Jiménez-Alfaro, S.M. Hennekens, Z. Botta-Dukát, M. Chytrý, R. Field, F. Jansen, … & U. Jandt 2018. Global trait – environment relationships of plant communities. Nature *Ecology & Evolution* 2:1906–1917.

Carlquist, S. J. 2001. *Comparative wood anatomy, systematic, ecological, and evolutionary aspects of dicotyledon wood*. 2nd ed. Springer Series in Wood Science, Berlin, 448 pp.

Chavchavadze, E.S. & O.Yu. Sizonenko 2002. *Structural features of wood of shrubs and dwarf shrubs of the Arctic flora of Russia*. Rostok, St. Petersburg, 272 pp. (in Russian). [Чавчавадзе Е.С., Сизоненко О.Ю. 2002. Структурные особенности древесины кустарников и кустарничков арктической флоры России. Санкт-Петербург: Росток. 272 с.].

Chen, Z., S. Zhu, Y. Zhang, J. Luan, S. Li, P. Sun, X. Wan & S. Liu 2020. Tradeoff between storage capacity and embolism resistance in the xylem of temperate broadleaf tree species. *Tree Physiology* 40:1029–1042.

Clerx, L.E., F.E. Rockwell, J.A. Savage & N.M. Holbrook 2020. Ontogenetic scaling of phloem sieve tube anatomy and hydraulic resistance with tree height in *Quercus rubra*. *American Journal of Botany* 107:852–863.

De Schepper, V., T. De Swaef, I. Bauweraerts & K. Steppe 2013. Phloem transport: a review of mechanisms and controls. *Journal of Experimental Botany* 64(16):4839–4850.

Eryomin, V.M. 1982. Features of the anatomical structure of the bark of some Pinaceae in connection with the growth conditions. *Lesnoi Zhurnal* 3:14–18 (in Russian). [Еремин В.М., 1982. Особенности анатомического строения коры некоторых видов Pinaceae в связи с условиями произрастания // Лесной журнал. Вып. 3. С. 14–18].

Eryomin, V.M. 1983. *Comparative bark anatomy of Pinaceae*. Doctoral thesis, Voronezh State University, Voronezh (in Russian). [Еремин В.М. 1983. Сравнительная анатомия сосновых. Диссертация на соискание ученой степени доктора биологических наук. Воронеж].

Eryomin, V.M. & A.V. Kopanina 2012. *Atlas of the bark anatomy of trees, shrubs and lianas of Sakhalin and the Kuril Islands*. Poligrafica, Brest, 896 pp. (in Russian). [Еремин В.М., Копанина А.В. 2012. Атлас анатомии коры деревьев, кустарников и лиан Сахалина и Курильских островов. Брест: Полиграфика. 896 с.].

Esau, K. 1953. *Plant anatomy*. Chapman & Hall, London, 735 pp.

Esau, K. 1965. Anatomy and cytology of *Vitis* phloem. *Hilgardia* 37:17–72.

Esau, K. 1977. *Anatomy of the seed plants. 2nd ed*. John Wiley & Sons Ltd, New York, 576 pp.

Evert, R.F. 2006. *Esau's plant anatomy: meristems, cells, and tissues of the plant body – their structure, function, and development*. Wiley, Hoboken, New Jersey, 624 pp.

Furze, M.E., S. Trumbore & H. Hartmann 2018. Detours on the phloem sugar highway: stem carbon storage and remobilization. *Current Opinion in Plant Biology* 43:89–95.

Gamalei, Yu.V. 2004. *Transport system of vascular plants. Origin, structure, functions, development, analysis of type diversity along the taxonomical and eco-geographical groups of plants, evolution and ecological specialization of transport system*. Saint Petersburg University, St. Petersburg, 421 pp. (in Russian). [Гамалей Ю.В. 2004. Транспортная система сосудистых растений. Происхождение, структура, функции, развитие, анализ разнообразия типов по таксономическим и эколого-географическим группам растений, эволюция и экологическая специализация транспортной системы. Санкт-Петербург: Санкт-Петербургский университет. 421 с.].

Gladkova, G.A & G.K. Butovets 1988. Volcanic soils of Kunashir Island. *Pochvovedenie* 2:54–67 (in Russian). [Гладкова Г.А., Бутовец Г.К. 1988. Вулканические почвы острова Кунашир // Почвоведение. № 2. С. 54–67].

Goldfarb, I.L. 2005. *Effect of hydrothermal activity on the conditions of pedogenesis (by the example of Kamchatka)*. Candidate Thesis. Lomonosov Moscow State University, Moscow, 24 pp. (in Russian). [Гольдфарб И.Л. 2005. Влияние гидротермального процесса на почвообразование

(на примере Камчатки): Автореф. дис. ... канд. геогр. наук. Москва: МГУ им. М.В. Ломоносова. 24 с.].

Gorshkov, G.S. 1967. *Volcanism of the Kuril island arc*. Nauka, Moscow, 183 pp. (in Russian). [Горшков Г.С. 1967. Вулканизм Курильской островной дуги. М.: Наука. 183 с.].

Gričar, J. 2024. Phloem: a missing link in understanding tree growth response in a changing environment. *Journal of Experimental Botany* 75(22): 6898–6902.

Grishin, S.Yu. 2003. The largest volcanic eruptions of the twentieth century in Kamchatka and the Kuril Islands and their impact on vegetation. *Izvestiya Russkogo geograficheskogo obshchestva* 135(3):19–28 (in Russian). [Гришин С.Ю. 2003. Крупнейшие вулканические извержения XX столетия на Камчатке и Курильских островах и их влияние на растительность // Известия Русского географического общества. Т. 135. Вып. 3. С. 19–28].

Grishin, S.Yu., P.A. Perepelkina & M.L. Burdukovskiia 2019. Beginning of vegetation succession on lava flows from the 2012–2013 eruption of Tolbachik volcano, Kamchatka. *Russian Journal of Ecology* 50(3):226–229.

Hartmann, H. & S. Trumbore 2016. Understanding the roles of nonstructural carbohydrates in forest trees – from what we can measure to what we want to know. *New Phytologist* 211:386–403.

Holbrook, N.M. & M. Knoblauch 2018. Editorial overview: Physiology and metabolism: Phloem: a supracellular highway for the transport of sugars, signals, and pathogens. *Current Opinion in Plant Biology* 43:1–4.

Hölttä, T., M. Mencuccini & E. Nikinmaa 2009. Linking phloem function to structure: Analysis with a coupled xylem–phloem transport model. *Journal of Theoretical Biology* 259:325–337.

Huang, C.-W., J.-C. Domec, S. Palmroth, W.T. Pockman, M.E. Litvak & G.G. Katul 2018. Transport in a coordinated soil–root–xylem–phloem leaf system. *Advances in Water Resources* 119:1–16.

Inagawa, T., T. Riutta, N. Majalap-Lee, R. Nilus, J. Josue & Y. Malhi 2023. Radial and vertical variation of wood nutrients in Bornean tropical forest trees. *Biotropica* 55:1019–1032.

Jyske T. & T. Hölttä 2015. Comparison of phloem and xylem hydraulic architecture in *Picea abies* stems. *New Phytologist* 205:102–115.

Kabanov, N.E. 1972. *Stone-birch forests in botanical-geographical and silvicultural relations*. Nauka, Moscow, 136 pp. (in Russian). [Кабанов Н.Е. 1972. Каменноберезовые леса в ботанико-географическом и лесоводственном отношениях. М.: Наука. 136 с.].

Kawai, K., K. Minagi, T. Nakamura, S.-T. Saiki, K. Yazaki & A. Ishida, 2021. Parenchyma underlies the interspecific variation of xylem hydraulics and carbon storage across 15 woody species on a subtropical island in Japan. *Tree Physiology* 42:337–350.

Khan, K.K., Z. Ahmad & M. Iqbal 1981. Trends of ontogenetic size variation of cambial initials and their derivatives in the stem of *Bauhinia parviflora* Vahl. *Bulletin de la Société Botanique de France. Lettres Botaniques*. 128(3):165–175.

Kopanina, A.V. 2019 Structural features of bark and wood of *Spiraea beauverdiana* (Rosaceae) in the extreme conditions of Arctic and volcanic activity on the Kuril Islands. *Sibirskii Lesnoi Zhurnal* 3:52–63 (in Russian with English abstract). [Копанина А.В. 2019. Структурные особенности коры и древесины *Spiraea beauverdiana* (Rosaceae) в экстремальных условиях Арктики и поствулканической активности на Курильских островах // Сибирский лесной журнал. № 3. С. 52–63].

Kopanina, A.V., I.I. Vlasova & E.O. Vatserionova 2017. Structural adaptation of woody plants to the conditions of volcanic landscapes of the Kuril Islands. *Vestnik DVO RAN* 1:88–96 (in Russian with English abstract). [Копанина А.В., Власова И.И., Вацерионова Е.О. 2017. Структурные адаптации древесных растений к условиям вулканических ландшафтов Курильских островов // Вестник ДВО РАН. № 1. С. 88–96].

Kopanina, A.V. & I.I. Vlasova 2019. Structural changes of bark of the woody liana *Toxicodendron orientale* Greene (Anacardiaceae) in the extreme environments of gas-hydrothermal volcanic activity. *Botanica Pacifica* 8(2):3–17.

Kopanina, A.V., E.V. Lebedeva & I.I. Vlasova 2020. Structural traits of woody plants and geomorphological conditions to the vegetation recovery at Ksudach caldera (Southern Kamchatka) since the explosive eruption in 1907. *Journal of Mountain Science* 17(7):1613–1635.

Kopanina, A.V.,·A.I. Talskikh, I.I. Vlasova & E.L. Kotina 2022. Age-related pattern in bark formation of *Betula ermanii* growing in volcanic environments from southern Sakhalin and Kuril Islands (Northeast Asia). *Trees: Structure and Function* 36:915–939.

Korablev, A.P. & V.Yu. Neshataeva 2016. Primary plant successions of forest belt vegetation on the Tolbachinskii Dol volcanic plateau (Kamchatka). *Biology Bulletin* 43(4):307–317.

Korablev, A.P., E.V. Sandalova, K.A. Arapov & K.M. Zaripova 2024. Biomorphological traits and leaf dry matter content are important to plant persistence in a highly unstable volcanic ground. *Nature Conservation Research* 9(2):73–89.

Korablev, A.P., V.E. Smirnov, V.Yu. Neshataeva & L.G. Khanina 2018. Plant life-forms and environmental filtering during primary succession on loose volcanic substrata (Kamchatka, Russia). *Biology Bulletin* 45(3):255–264.

Krestov, P.V. 2003. Forest vegetation of the easternmost Russia (Russian Far East). In: *Forest vegetation of Northeast Asia* (J. Kolbek, M. Šrůtek, E.O. Box, eds), pp. 93–180, Springer, Netherlands.

Laverov, N.P., N.L. Dobretsov, O.A. Bogatikov, V.G. Bondur, A.G. Gurbanov, B.S. Karamurzov, V.I. Kovalenko, I.V. Melekestsev, S.E. Nechaev, V.V. Ponomareva, ... & V.V. Yarmolyuk 2005. *The newest and modern volcanism in Russia*. Nauka, Moscow, 604 pp. (in Russian). [Лаверов Н.П., Добрецов Н.Л., Богатиков О.А., Бондур В.Г., Гурбанов А.Г., Карамурзов Б.С., Коваленко В.И., Мелекесцев И.В., Нечаев Ю.В., Пономарева В.В., ... Ярмолюк В.В. 2005. Новейший и современный вулканизм на территории России. Москва: Наука. 604 с.].

Levionnois, S., C. Ziegler, P. Heuret, S. Jansen, C. Stahl & E. Calvet 2021. Is vulnerability segmentation at the leaf-stem transition a drought resistance mechanism? A theoretical test with a trait-based model for Neotropical canopy tree species. *Annals of Forest Science* 78:87.

Lev-Yadun, S. 2025. Regulating the vascular cambium: do not forget the vascular ray initials and their derivatives. *Plants* 14:592.

Lev-Yadun, S. & R. Aloni 1990. Polar patterns of periderm ontogeny, their relationship to leaves and buds, and the control of cork formation. *IAWA Bulletin* 11:289–300.

Li, S., X. Li, R. Link, R. Li, L. Deng, B. Schuldt, X. Jiang, R. Zhao, J. Zheng, S. Li & Y. Yin, 2019. Influence of cambial age and axial height on the spatial patterns of xylem traits in *Catalpa bungei*. *Forests* 10:662.

Li, P.C. & A.K. Skvortsov 1999. Betulaceae Gray. In: *Flora of China, vol. 4* (Z.Y. Wu & P.H. Raven, eds), pp. 286–313, Science Press, Beijing; Missouri Botanical Garden Press, St. Louis.

Liesche, J., M.R. Pace, Q. Xu, Y. Li & S. Chen 2016. Height-related scaling of phloem anatomy and the evolution of sieve element end wall types in woody plants. *New Phytologist* 214(1):14360.

Liesche, J. & A. Schulz 2018. Phloem transport in gymnosperms: A question of pressure and resistance. *Current Opinion in Plant Biology* 43:36–42.

Lintunen, A., T. Paljakka, T. Jyske, M. Peltoniemi, F. Sterck, G. von Arx, H. Cochard, P. Copini, M.C. Caldeira, S. Delzon, ... & T. Hölttä 2016. Osmolality and non-structural carbohydrate composition in the secondary phloem of trees across a latitudinal gradient in Europe. *Frontiers in Plant Science* 7:726.

Losada, J. M., & Holbrook, N. M. 2019. Scaling of phloem hydraulic resistance in stems and leaves of the understory angiosperm shrub *Illicium parviflorum*. *American Journal of Botany* 106:244–259.

Manko, Yu.I. & A.N. Sidelnikov 1989. *Effect of volcanism on vegetation*. DVO AN SSSR, Vladivostok, 164 pp. (in Russian). [Манько Ю.И., Сидельников А.Н. 1989. Влияние вулканизма на растительность. Владивосток: ДВО АН СССР. 164 с.].

Manko, Yu.I. 1967. *Fir-spruce forests of the northern Sikhote-Alin. Natural regeneration, structure and development*. Nauka, Leningrad, 244 pp. (in Russian). [Манько Ю.И. 1967. Пихтово-еловые леса северного Сихотэ-Алиня. Естественное возобновление, строение и развитие. Л.: Наука. 244 с.].

Manko, Yu.I. 1980. Volcanism and dynamics of vegetation. *Botanicheskii Zhurnal* 65(4):457–469 (in Russian). [Манько Ю.И. 1980. Вулканизм и динамика растительности // Ботанический журнал. Т. 65, № 4. С. 457–469].

McClelland, L. (ed.) 1992. Global volcanism program. Report on Sashiusudake [Baransky]. *Smithsonian Institution Bulletin of the Global Volcanism Network* 17:12.

McCubbin, T.J. & D.M. Braun 2021. Phloem anatomy and function as shaped by the cell wall. *Journal of Plant Physiology* 266:153526

Meng, Q., F. Fu, J. Wang, T. He, X. Jiang, Y. Zhang, Y. Yin, N. Li & J. Guo 2021. Ray traits of juvenile wood and mature wood: *Pinus massonia* and *Cunninghamia lanceolata*. *Forests* 12:1277.

Miyawaki, A. 1985. *Vegetation of Japan. Vol. 6*. Chubu, Shibundo, Tokyo, 604 pp. (in Japanese with German summary).

Molina, J.G.A., M.A. Hadad, D.P. Domínguez & F.A. Roig 2016. Tree age and bark thickness as traits linked to frost ring probability on *Araucaria araucana* trees in northern Patagonia. *Dendrochronologia* 37:116–125.

Morris, H., M.A.F. Gillingham, L. Plavcová, S.M. Gleason, M.E. Olson, D.A. Coomes, E. Fichtler, M.M. Klepsch, H.I. Martínez-Cabrera, D.J. McGlinn, ... & S. Jansen 2018. Vessel diameter is related to amount and spatial arrangement of axial parenchyma in woody angiosperms. *Plant, Cell & Environment* 41:245–260.

Nardini, A., M.A. Lo Gullo & S. Salleo 2011. Refilling embolized xylem conduits: Is it a matter of phloem unloading? *Plant Science* 180(4):604–611.

Nedoluzhko, A.K. & A.K. Skvortsov 1996. Fam. Berezovye – Betulaceae In: *Vascular plants of the soviet Far East, vol. 8* (S.S. Kharkevich, ed.), pp. 13–24, Nauka, St. Petersburg (in Russian). [Недолужко А.К., Скворцов А.К. 1996. Семейство Березовые – Betulaceae // Сосудистые растения советского Дальнего Востока / отв. ред. С.С. Харкевич. Санкт-Петербург: Наука. Т. 8. С. 13–24].

Neshataeva, V.Yu. 2009. *Vegetation of the Kamchatka Peninsula*. KMK Scientific Press Ltd., Moscow, Russia. 537 pp. (in Russian). [Нешатаева В.Ю. 2009. Растительность полуострова Камчатка. Москва: Товарищество научных изданий КМК. 237 с.].

Neshataeva, V.Yu., A.O. Pesterov & A.P. Korablev 2021. *Vegetation of the volcanic belt of Kamchatka (within the Kronotsky Reserve)*. Marafon, St. Petersburg, 328 pp. (in Russian). [Нешатаева В.Ю., Пестеров А.О., Кораблев А.П. 2021. Растительность вулканического пояса Камчатки (в пределах Кроноцкого заповедника). Санкт-Петербург: Марафон. 328 с.].

Ohwi, J. 1965. *Flora of Japan*. Smithsonian Institution, Washington, 1067 pp.

Olson, M.E. 2020. From Carlquist's ecological wood anatomy to Carlquist's Law: why comparative anatomy is crucial for functional xylem biology. *American Journal of Botany* 107:1328–1341.

Olson, M.E., T. Anfodillo, S.M. Gleason & K.A. McCulloh 2021. Tip-to-base xylem conduit widening as an adaptation: causes, consequences, and empirical priorities. *New Phytologist* 229: 1877–1893.

Onyenedum, J.G. & M.R. Pace 2021. The role of ontogeny in wood diversity and evolution. *American Journal of Botany* 108(12):1–25.

Pace, M.R. & V. Angyalossy 2013. Wood anatomy and evolution: a case study in the Bignoniaceae. *International Journal of Plant Sciences* 174:1014–1048.

Pace, M.R., L.G. Lohmann, R.G. Olmstead & V. Angyalossy 2015. Wood anatomy of major Bignoniaceae clades. *Plant Systematics and Evolution* 301: 967–995.

Pace, M.R., V. Angyalossy, P. Acevedo-Rodríguez & J. Wen 2018. Structure and ontogeny of successive cambia in *Tetrastigma* (Vitaceae), the host plants of Rafflesiaceae. *Journal of Systematics and Evolution* 56:394–400.

Park, Y.I.D., A. Koubaa, S. Brais & M.J. Mazerolle 2009. Effects of cambial age and stem height on wood density and growth of jack pine grown in boreal stands. *Wood and Fiber Science* 41:346–358.

Petit, G. & A. Crivellaro 2014. Comparative axial widening of phloem and xylem conduits in small woody plants. *Trees* 28:915–921.

Pfautsch, S., T. Hölttä & M. Mencuccini 2015. Hydraulic functioning of tree stems–fusing ray anatomy, radial transfer and capacitance. *Tree Physiology* 35:706–722.

Plavcova, L. & S. Jansen 2015. The role of xylem parenchyma in the storage and utilization of nonstructural carbohydrates. *Functional and Ecological Xylem Anatomy* 26:209–234.

Plavcova, L., G. Hoch, H. Morris, S. Ghiasi & S. Jansen 2016. The amount of parenchyma and living fibers affects storage of nonstructural carbohydrates in young stems and roots of temperate trees. *American Journal of Botany* 103(4):603–612.

Plavcová, L., V. Jandová, J. Altman, P. Liancourt, K. Korznikov & J. Doležal 2024. Variations in wood anatomy in Afrotropical trees with a particular emphasis on radial and axial parenchyma. *Annals of Botany* 134:151–162.

Prozina, M.N. 1960. *Botanical micro-technics*. Vysshaya shkola, Moscow, 206 pp. (in Russian). [Прозина М.Н. 1960. Ботаническая микротехника. М.: Высшая школа. 206 с.].

Quilhó, T., H. Pereira & H.G. Richter 2000. Within-tree variation in phloem cell dimensions and proportions in *Eucalyptus globulus*. *IAWA Journal* 21:31–40.

Richardson, A.D., M.S. Carbone, T.F. Keenan, C.I. Czimczik, D.Y. Hollinger, P. Murakami, P.G. Schaberg & X. Xu 2013. Seasonal dynamics and age of stemwood nonstructural carbohydrates in temperate forest trees. *New Phytologist* 197:850–861.

Rosell, J.A., S. Gleason, R. Mendez-Alonzo, Y. Chang & M. Westoby 2014. Bark functional ecology: evidence for tradeoffs, functional coordination, and environment producing bark diversity. *New Phytologist* 201:486–497.

Rosell, J.A., F.I. Piper, C. Jiménez-Vera, P.C.B. Vergílio, C.R. Marcati, M. Castorena & M.E. Olson 2020. Inner bark as a crucial tissue for non-structural carbohydrate storage across three tropical woody plant communities. *Plant, Cell & Environment* 44(1):156–170.

Rungwattana, K. & P. Hietz 2018. Radial variation of wood functional traits reflects size-related adaptations of tree mechanics and hydraulics. *Functional Ecology* 32:260–272.

Samkova, T.Yu. 2009. *Influence of the hydrothermal process on vegetation (the example of the Pauzhetskaya hydrothermal system of Kamchatka)*. Candidate Thesis. Institute of Volcanology and Seismology FEB RAS, Petropavlovsk-Kamchatsky, 24 pp. (in Russian). [Самкова Т.Ю. 2009. Влияние гидротермального процесса на растительность (на примере Паужетской гидротермальной системы Камчатки): Автореф. дис. … канд. биол. наук. Петропавловск-Камчатский: ИВиС ДВО РАН. 24 с.].

Samkova, T.Yu., S.A. Rylova & E.S. Klyapitsky 2016. Spatial heterogeneity of the thermal field and its reflection in the structure of vegetation cover of the southeastern part of the Bolshe-Bannoye deposit (Southern Kamchatka) *Vestnik KRAUNTS. Nauki o Zemle* 31(3):18–27 (in Russian with English abstract). [Самкова Т.Ю., Рылова С.А., Кляпицкий Е.С. 2016. Пространственная неоднородность термального поля и ее отражение в структуре растительного покрова юго-восточного участка Большe-Банного месторождения (Южная Камчатка) // Вестник КРАУНЦ. Науки о Земле. Вып. 31, № 3. С. 18–27].

Savage, J.A., S.D. Beecher, L. Clerx, J.T. Gersony, J. Knoblauch, J.M. Losada, K.H. Jensen, M. Knoblauch & N.M. Holbrook 2017. Maintenance of carbohydrate transport in tall trees. *Nature Plants* 3:965–972.

Schröter, D.M. & W. Oberhuber 2021. Do growth-limiting temperatures at the high-elevation treeline require an adaptation of phloem formation and anatomy? *Frontiers in Forests and Global Change* 4:731903.

Sellier, D. & J.J. Harrington 2014. Phloem transport in trees: A generic surface model. *Ecological Modelling* 290:102–109.

Sevanto, S. 2018. Drought impacts on phloem transport. *Current Opinion in Plant Biology* 43:76–81.

Shemberg, M.A. 1986. *Stone birch: taxonomy, geography, variability*. Nauka, Novosibirsk, 175 pp. (in Russian). [Шемберг М.А. 1986. Береза каменная: систематика, география, изменчивость. Новосибирск: Наука. 174 с.].

Shtein, I., J. Gričar, S. Lev-Yadun, A. Oskolski, M.R. Pace, J.A. Rosell & A. Crivellaro 2023. Priorities for bark anatomical research: study venues and open questions. *Plants* 12:1985.

Skripalshchikova, L.N., V.V. Stasova, V.D. Perevoznikova, O.N. Zubareva & A.I. Tatarintsev 2009. Effect of the complex of technogenic and recreational loads on development of trunk tissues of scotch pine in the Krasnoyarsk forest-steppe. *Biology Bulletin* 36(5):524–531.

Skvortsov, A.K., G.N. Ogureeva, O.A. Svyazeva & S.Ya. Sokolov 1977. The genus *Betula* L. – Birch. In: *Areals of trees and shrubs in the USSR. Part 1*, (A.K. Skvortsov, ed.), pp. 89–100, Nauka, Leningrad (in Russian). [Скворцов А.К., Огуреева Г.Н., Связева О.А., Соколов С.Я. 1977. Род *Betula* L. – Береза // Ареалы деревьев и кустарников. СССР / под ред. А.К. Скворцова. Ленинград: Наука. Ч. 1. С. 89–100.].

Sokolov, I.A. 1973. *Volcanism and soil formation*. Nauka, Moscow, 224 pp. (in Russian). [Соколов И.А. 1973. Вулканизм и почвообразование. Москва: Наука. 224 с.].

Spicer, R. & B. Gartner 2001. The effects of cambial age and position within the stem on specific conductivity in Douglas-fir (*Pseudotsuga menziesii*) sapwood. *Trees* 15:222–229.

Stasova, V.V., L.N. Skripalshikova, O.N. Zubareva & A.I. Tatarintsev 2011. Structure and development of stem tissues of *Betula pendula* (Betulaceae) under the anthropogenic pollution. *Rastitelnye Resursy* 47(2):66–75 (in Russian with English abstract). [Стасова В.В., Скрипальщикова Л.Н., Зубарева О.Н, Татаринцев А.И. 2011. Строение и развитие тканей ствола *Betula pendula* (Betulaceae) в условиях антропогенного загрязнения // Растительные ресурсы. Т. 47, № 2. С 66–75].

Stasova, V.V., L.N. Skripalschikova, O.P. Secretenko, A.I. Tatarintsev & M.A. Plyashechnik 2013. The effect of heavy metals on the structure of wood in *Betula pendula* (Betulaceae) in technogeneously disturbed landscapes in Krasnoyarsk forest-steppe. *Rastitelnye Resursy* 49(4):532–541 (in Russian with English abstract). [Стасова В.В., Скрипальщикова Л.Н., Секретенко О.П., Татаринцев А.И., Пляшечник М.А. 2013. Влияние тяжелых металлов на структуру древесины *Betula pendula* (Betulaceae) в техногеннонарушенных ландшафтах красноярской лесостепи // Растительные ресурсы. Т. 49, № 4. С. 532–541].

Stasova, V.V., O.N. Zubareva, G.A. Ivanova & A.B. Bazhenova 2020. Postfire changes of inner bark in Scots pine stems. *Sibirskii Lesnoi Zhurnal* 5:14–27 (in Russian with English abstract). [Стасова В.В., Зубарева О.Н., Иванова Г.А., Баженова А.Б. 2020. Постпирогенные изменения луба ствола сосны обыкновенной // Сибирский лесной журнал. № 5. С. 14–27].

Steppe, K., F. Sterck & A. Deslauriers 2015. Diel growth dynamics in tree stems: linking anatomy and ecophysiology. *Trends in Plant Science* 20:335–343.

Talskih, A.I., A.V. Kopanina & I.I. Vlasova 2022. Features of the structural response of the bark and wood of birch (*Betula platyphylla*, Betulaceae) in the landscapes of sea coasts, magmatic and mud volcanoes of Sakhalin and the Kuril Islands. *Geosistemy Perehodnykh Zon* 6(4):360–379 (in Russian with English abstract). [Тальских А.И., Копанина А.В., Власова И.И. 2022. Особенности структурного отклика коры и древесины березы плосколистной (*Betula platyphylla*, Betulaceae) в ландшафтах морских побережий, магматических и грязевых вулканов Сахалина и Курильских островов // Геосистемы переходных зон. Т. 6, № 4. С. 360–379].

Tarelkina, T.V., A.A. Serkova, N.A. Galibina, E.V. Novichonok, S.A. Moshnikov, D.S. Ivanova & L.I. Semenova 2024. Estimation of phloem conductance at tree level in young, middle-aged and old-aged Scots pine trees growing in different climatic conditions in boreal forests. *Tree Physiology* 44(8):081

Thompson, M.V. 2006. Phloem: the long and the short of it. *Trends in Plant Science* 11(1):26–32.

Trockenbrodt, M. 1991. Qualitative structural changes during bark development in *Quercus robur, Ulmus glabra*, *Populus tremula* and *Betula pendula*. *IAWA Bulletin* 12:5–22.

Tsuchiya, R. & I. Furukawa 2010. Relationship between the radial variation of ray characteristics and the stages of

radial stem increment in *Zelkova serrata*. *Journal of Wood Science* 56:495–501.

Van Bel, A.J.E. 2021. The plant axis as the command centre for (re)distribution of sucrose and amino acids. *Journal of Plant Physiology* 265:153488.

Vandegehuchte, M.W., J. Bloemen, L.L. Vergeynst & K. Steppe 2015. Woody tissue photosynthesis in trees: salve on the wounds of drought? *New Phytologist* 208(4):998–1002.

IVS FEB RAS Geoportal. *VOKKLA (Volcanoes of Kurile-Kamchatka Island Arc): Volcano Baransky*. Available from: http://geoportal.kscnet.ru/volcanoes/volc?ln=bib&name=Baransky Last accessed: 15.01.2024.

von Arx, G., J.M. Olano & P. Fonti 2015. Assessing conifer ray parenchyma for ecological studies: pitfalls and guidelines. *Frontiers in Plant Science* 6:1016.

Wittmann, C. & H. Pfanz 2007. Temperature dependency of bark photosynthesis in beech (*Fagus sylvatica* L.) and birch (*Betula pendula* Roth.) trees. *Journal of Experimental Botany* 58:4293–4306.

Woodruff, D.R. 2014. The impacts of water stress on phloem transport in Douglas-fir trees. *Tree Physiology* 34:5–14.

Yatsenko-Khmelevsky, A.A. 1954. *Fundamentals and methods of wood anatomical research*. AN SSSR, Leningrad, Moscow. 337 pp. (in Russian). [Яценко-Хмелевский А.А. 1954. Основы и методы анатомического исследования древесины. Ленинград; Москва: АН СССР. 337 с.].

Zakharikhina, L.V. & Yu.S. Litvinenko 2019. Volcanism and geochemistry of the soil and plant cover in Kamchatka. Part 2. The formation of the elemental composition of volcanic soils under cold humid conditions. *Journal of Seismology and Volcanology* 13(3):149–156.

Zhang, F., Y.-W. Liu, J. Qin, S. Jansen, S.-D. Zhu & K.-F. Cao 2024. Xylem embolism induced by freeze–thaw and drought are influenced by different anatomical traits in subtropical montane evergreen angiosperm trees. *Physiologia Plantarum* 176(5):e14567.

Zharkov, R.V. 2014. *Thermal sources of southern Kuril Islands*. Dalnauka, Vladivostok, 378 pp. (in Russian). [Жарков Р.В. 2014. Термальные источники Южных Курильских островов. Владивосток: Дальнаука. 378 с.].